DOE/NASA/0022-2
NASA CR-165158
SRC-80TR-62

NASA-CR-165158
19810004848

MEASUREMENT OF ROD SEAL LUBRICATION FOR STIRLING ENGINE APPLICATION

Allan I. Krauter
Shaker Research Corporation

July 1980

Prepared for
NATIONAL AERONAUTICS AND SPACE ADMINISTRATION
Lewis Research Center
Under Contract DEN 3-22

for
U.S. DEPARTMENT OF ENERGY
Conservation and Solar Applications
Office of Transportation Programs

NOTICE

ERRATA

NASA Contractor Report 165157
DOE/NASA/0022-2
SRC-80TR-62

MEASUREMENT OF ROD SEAL LUBRICATION

FOR STIRLING ENGINE APPLICATION

Allan I. Krauter
July 1980

The NASA Contractor Report number should be 165158.

On the last page, the Distribution Statement in block 18 should read

Unclassified - unlimited
STAR Category 37
DOE Category UC-96

DOE/NASA/0022-2
NASA CR-165157

MEASUREMENT OF ROD SEAL LUBRICATION FOR STIRLING ENGINE APPLICATION

Allan I. Krauter
Shaker Research Corporation
Ballston Lake, New York 12019

July 1980

Prepared for
National Aeronautics and Space Administration
Lewis Research Center
Cleveland, Ohio 44135
Under Contract DEN 3-22

for
U.S. DEPARTMENT OF ENERGY
Conservation and Solar Applications
Office of Transportation Programs
Washington, D.C. 20545
Under Interagency Agreement EC-77-A-31-1040

TABLE OF CONTENTS

LIST OF FIGURES

SUMMARY

This report presents the results of an experimental-analytical program concerned with the elastohydrodynamic behavior of sliding elastomeric seals for the Stirling engine. The objective of the program was to increase knowledge of elastomeric seal operation in a reciprocating application. To do this an experimental apparatus was designed and built and a detailed analysis was developed. The analysis determines the instantaneous oil film thickness throughout the cyclic reciprocating motion. The experimental apparatus allows seal leakage, seal friction, and oil film thickness to be measured. The oil film thickness measurement is made with a specially-developed optical interferometric procedure.

Tests were conducted on two commercial elastomeric seals: a "T" seal (76 mm O.D. and 3.8 mm between backing rings) and an "O" ring (76 mm O.D. and 5.3 mm diameter). Testing conditions included seal durometers of 70 and 90, sliding velocities of 0.8, 2.0, and 3.6 m/s, and no pressure gradient across the seal. Both acrylic and aluminum cylinders were used. Measured oil film thickness profiles were compared to results of the elastohydrodynamic analysis. The comparison shows an overall qualitative agreement. Friction and oil leakage measurements were also made at these sliding speeds. The fluid used was a typical synthetic base automotive lubricant.

It is concluded that this first time experimental-analytical comparison for oil film thickness indicates the need for some improvements in the analytical model and in the experimental technique.

INTRODUCTION

The performance of seals is important to the efficiency and practicality of Stirling engines. One of these seals, the rod seal, has the function of separating the high pressure gas from the low or ambient pressure oil. For this seal, the gas leakage, oil leakage, and friction must be low. In addition, the life of the seal should be high. Producing these somewhat contradictory characteristics requires a basic understanding of the behavior of the seal. To provide this understanding, a technology effort, under sponsorship of the DOE through NASA, has been underway. This effort, under NASA Contract DEN3-22, has the objective of increasing present knowledge of elastomeric seal operation in a reciprocating application. The contract is concerned with applying hydrodynamic and elastohydrodynamic theory to the rod seal. The contract is also concerned with the experimental determination of film thickness, fluid leakage, and power loss. The contract entails the production of theoretical and experimental results, the comparison of these results, and the development of tools appropriate for evaluating rod seal behavior.

Increasing the knowledge of reciprocating elastomeric seal behavior has been the object of other recent investigations. For steady state sliding, recent analytical results include those of Herrebrugh [1]* for line contacts and those of Hamrock and Dowson [2] for low modulus point contacts. Both give expressions for the minimum film thickness in the contact zone. For squeeze film conditions Herrebrugh [3] gives an expression based on two normally approaching cylinders with an isoviscous lubricant. For the Stirling engine seal, both sliding and squeeze film effects are present. Results for this situation are presented in [4], which is the Interim Report for the present contract.

Experimentally, friction force and leakage measurements for reciprocating Stirling engine seal applications have been made by General Motors [5,6]. In these measurements, several seal designs were explored; however, no measurements of oil film thickness were made and no analytical-experimental film thickness comparisons were given. The variation of film profile in a rod seal during a reciprocating cycle was observed first by Blok and Koens [7] using an interferometric technique. Such variation was measured using a probe by Field and Nau [8]. It was found that measured friction was higher than that expected from film profile calculations. Several seal parameters which affect the behavior of the seal were identified. Investigations considering indirect effects of elastomeric seal operation have also been made. For example, Hirano and Murakami [9] give results of a photoelastic study of elastohydrodynamic contact conditions in reciprocating motion.

*Numbers in brackets denote references.

The most sensitive measurement of elastomeric seal operation is the oil film thickness distribution. This measurement can be made using optical interferometry, which gives the complete distribution in the contact zone. The major difficulty with the technique is producing the interference fringes. Roberts [10,11], produced these fringes by preparing special rubber specimens having optically smooth surfaces. Methods such as seal coating were used by others, including Blok and Koens [12] and Field and Nau [13].

The present work has been concerned with improving the existing analytical and experimental techniques for evaluating elastomeric seals during reciprocating motion. The work has also been concerned with a first-time application of the improved techniques. At the end of the first year of the two-year contract period, the techniques had been developed. Analytically, a computer program was produced. This program calculates the film thickness and contact pressure distributions as a function of the sinusoidal seal/cylinder motion. The program is based on a numerical EHD analysis of low modulus line contacts. Included in the analysis are a Hertzian seal preload, fully flooded conditions, and no externally applied axial pressure gradient. Also during the first year, an experimental apparatus was designed, constructed, and tested. The apparatus contains a moving transparent cylinder (for interferometric measurement of oil film thickness) and a stationary elastomeric test seal. This arrangement, rather than the conventional one in which the cylinder is stationary and the rod moves, was selected to allow non-moving optics and relatively easy optical access to the seal. The apparatus operates in the range 10 to 50 Hz and has a 25 mm (1 in.) total stroke. The features of the apparatus include a built-in force cell for seal friction measurements, ease of seal and cylinder replacement, water cooling, balanced inertial forces, and precise guidance of the cylinder by hydrostatic oil bearings.

Both the computer program (including the supporting analysis) and the experimental apparatus are presented and described in an Interim Report [4]. That report, which was written at the end of the first year, also contains results obtained from numerous runs of the computer program.

The present report is intended to describe the contract work that occurred since the Interim Report was issued. As a result, this report does not repeat material already included in [4]; instead, that report is referenced frequently. It is suggested that the reader who is interested in technical details of the present report have a copy of [4] available.

The present report contains, in the next section, a discussion of the modifications made to the experimental apparatus during the past year. In the following section, the experimental scope is

presented. This scope covers the measurement of leakage, friction, and oil film thickness distribution and the seal parameters considered. These parameters include cylinder surface finish, seal design, frequency, preload, and duration of the test. The techniques used to make the measurements and tests and the testing conditions are described next, including a detailed discussion of the optical interferometric procedure developed under the contract.

The experimental results section contains results for friction force and leakage, for the 10 hour test, and for oil film thickness. The film thickness results are given first photographically, and then in terms of oil film thickness profiles. The photographs are also used to indicate what procedures are used in obtaining these profiles. Finally, experimental-analytical comparisons are made and a discussion of the results is presented.

The remaining sections contain a summary of results and references. Two short appendices contain the computer program used to determine characteristics of the optical interferometric technique and the procedure used in operating the experimental apparatus.

EXPERIMENTAL REPORT

Experimental Apparatus

This section describes the modifications to the experimental apparatus made since the Interim Report [4] was issued. These modifications include:

- substitution of a replaceable acrylic cylinder for the Lexan cylinder.
- fabrication and installation of a new test seal holder for the plunger.
- construction of a light guide having a rectangular cross-section.
- design, manufacture, and installation of hardware to synchronize the light flash to the stroke position.

With the exception of these modifications, the experimental apparatus was not changed from that shown in [4]. Specifically, the description given in the photographic figures (Figures 1, 2, 4, 5, and 7 of [4]) remain applicable to the apparatus as used for the present work.

Acrylic Cylinder

The Interim Report [4] discussed problems associated with the Lexan cylinder that was originally intended for use in the experimental apparatus. These problems included poor optical quality, difficulty in polishing, and softness which leads to early scratching. For these reasons, a commercially available acrylic tubing was obtained. This tubing has a 6.4 mm (0.25 in.) wall thickness and a 76 mm (3 in.) I.D. It is manufactured with polished inner and outer surfaces -- the only machining operations required prior to use are to cut the tubing to length, to square the ends, and to round the inner edge on one end for aiding the plunger installation. The acrylic cylinder can be inverted after scratching to double its useful life and can be replaced easily.

The acrylic tubing proved to be very suitable for the work performed. Although it is not sufficiently strong to contain 690 kPa (100 psi), it is relatively scratch resistant, sufficiently clear, and produces good optical interference fringes. For 690 kPa use, another acrylic cylinder having a 13 mm (1/2 in.) wall thickness was fabricated. That cylinder is not readily available commercially because its wall thickness at the 76 mm (3 in.) I.D. size is outside the standard range.

Test Seal Holder

A new test seal holder was deemed necessary for two reasons. Firstly, the stretching of the seal during installation tended to crack the optical coating on the seal. Secondly, the "T" seal being used

requires backing rings. These backing rings serve the purpose of minimizing extrusion of the rubber during high pressure applications. However, in the test apparatus, they were found to scratch the acrylic cylinder and make it optically useless in a short time (several minutes).

The new test seal holder (Figure 1) was designed to avoid both problems. Because it is in two pieces the seal need not be stretched during installation. Also, the axial groove width is sufficiently small that the seal is clamped slightly in the axial direction by the holder. This clamping effect, which is adjustable via shims at the central pilot, allows the seal to be operated without the backing rings. The clamping provides a secondary benefit -- the seal is held axially more securely as compared to the positioning produced with the backing rings. This better axial positioning is desirable because minimum axial seal motion is best to avoid blurring in the interference fringe photographs.

Light Guide

During the initial photographic work with the experimental apparatus, it became apparent that delivering sufficient light to the seal would be a significant problem. For that reason, a rectangular acrylic plate was made. The cross-section of the plate has dimensions 3 mm by 30 mm -- these correspond to the diameter and length of the camera flash tube being used. The length of the plate is about 130 mm (5 in.) which was determined by spacing of the camera flash, oscillating acrylic cylinder and camera. For the photographic work, the plate is positioned so that one end just contacts the tube of the camera flash and the other end just clears the oscillating acrylic cylinder. With this setup, a large proportion of light is captured from the flash and is delivered to the seal. (Further discussion of the optical setup is given in the following section.)

Synchronization Hardware

Special hardware was designed and built so that the camera flash could be triggered at a specific, known point of the cylinder motion. It was necessary that this hardware operate repeatably because the optical requirements dictate taking of multiple exposures. Such multiple exposures could result in blurred or indistinguishable fringes if the cyclic flash position is sufficiently random.

The synchronization hardware contains a stub shaft that is mounted to the shaft which drives the flywheel. On the stationary housing of this shaft is a light probe -- this light probe can be adjusted in its circumferential position. The light probe is targeted at a slot that is machined in the stub shaft. The pulse produced by the probe as its slot passes is processed, amplified, and transmitted to either an oscilloscope or to the camera flash. The camera flash

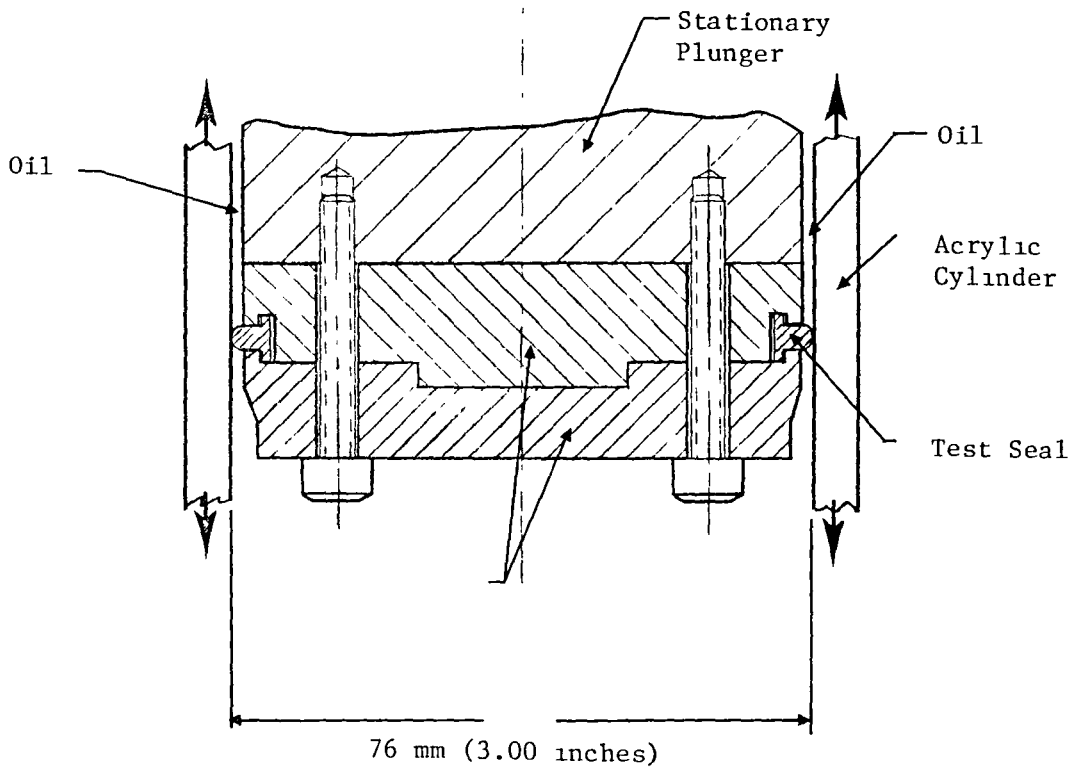

Figure 1 Schematic of Test Seal Holder

signal is transmitted only once each time a control button is pushed (this prevents sending a flash signal each time the slot for the flash signal probe passes).

Use of the synchronization hardware has shown that the flash point can be adjusted within a few degrees of the intended cyclic position. Once adjusted and fixed, the repeatability of the flash is well within a degree of the set position.

Experimental Scope

This section describes the scope of the experimental test program. The test program was intended to involve many of the parameters that influence elastomeric seal behavior. These parameters include:

- seal material and elastic modulus of the seal (70 or 90 durometer)*
- seal geometry (76 mm O.D. and 3.8 mm wide between backing rings for the "T" seal, 5.3 mm for the "O" ring)*
- frequency and stroke of oscillation (10 Hz, 25 Hz, or 50 Hz; 25.4 mm total stroke)*
- static preload on the seal (ratio, contact width to seal width, between 0.4 and 0.7)*
- temperature (normal ambient)*
- oil viscosity (0.4 Pa·s)*
- surface finish of the seal and of the cylinder (seal coated or uncoated; cylinder polished or unpolished)*
- pressure drop across the seal (0)*
- time – via changes in the above parameters (minutes or hours)*

A specific testing condition for the seal results when each of these parameters is fixed. The number of such conditions is obviously unlimited because of the number of potential combinations for the above parameters and because many of the parameters have continuously variable values. In addition, parameters such as seal geometry and surface finish are, in turn, themselves characterized by a large number of other parameters.

To develop a manageable test effort, it was necessary that a reasonable number of specific testing conditions be employed. The constraints of the contract work suggested that 10 such testing conditions would be sufficient for some experimental-analytical comparisons and also for providing some indication of general seal behavior. To produce these 10 testing conditions, the parameters were classified into groups. These groups are: Surface finish; Seal elasticity and design; Frequency; Preload; and Time.

The first group includes not only the surface finish of the seal and cylinder, but also the surface finish associated with coating of the seal. This coating, required by the optical technique used to measure

*Values used for testing (see Figure 2 and associated discussion).

the film thickness, has the potential for influencing the experimental results.

The second group includes the elastic modulus of the seal, the seal material, and the seal design. For the purpose of the tests conducted, the many parameters in this group were reduced to two seal designs and, for the first design, a "hard" and "soft" elastomeric material. The first seal is a "T" seal.* The second seal is an "O" ring.** The hard elastomeric material for the T seal is 90 durometer. The soft elastomeric material for the T seal is 70 durometer.

The third through fifth groups involve the vibration frequency, seal preload, and testing time, respectively.

The test matrix, which summarizes the tests run, is shown as Figure 2. Given on the figure are the 10 test conditions and the combinations from the five groups used to produce each test condition. The first test condition involves the acrylic cylinder, hard (90 durometer) T seal, 10 Hz oscillation frequency, low preload, and short time test. The second test condition is concerned with the influence of seal hardness (durometer) on the behavior of the seal. For this condition, the 90 durometer T seal is replaced with a 70 durometer T seal. This 70 durometer T seal is also used for test conditions 4-10. The third test condition is concerned with seal design -- for that condition an O ring is used instead of the T seal.

Test conditions 4 and 5 are concerned with oscillation frequency. For these conditions, oscillation frequencies of 25 and 50 Hz (rather than 10 Hz) are specified.

Test condition 6 is concerned with seal preload. Since specific preloads are difficult to produce, the general classifications of "low" and "high" preload are used (the actual preload attained is, however, one of the measured quantities for the tests).

Test conditions 7, 8, and 9 are associated with seal/surface finish. Specifically, the effect of removing the optical seal coating is treated via test number 7. In test number 8, the effect of changing the cylinder material is considered. Specifically, the acrylic cylinder is replaced with an aluminum cylinder for that test condition. Finally, in test 9, the effects of surface finish are studied by changing the surface finish of the aluminum cylinder.

Test 10 considers the effects of time (and associated variations of the various parametric values) on the behavior of the seal. For this

---

*The T seal is Parker No. TP032-4205 (low durometer) and TP032-4208 (high durometer). The backing rings for the seal are Nylon, Parker No. B001.

**The O ring is National No. 568-334.

Group	Description	Test Condition Number									
		1	2	3	4	5	6	7	8	9	10
1	Acrylic, Coated Seal Acrylic, Uncoated Seal Alum. (finish 1), Uncoated Seal Alum. (finish 2), Uncoated Seal	✓	✓	✓	✓	✓	✓	✓	✓	✓	✓
2	Hard T Seal Soft T Seal O Ring	✓	✓	✓	✓	✓	✓	✓	✓	✓	✓
3	Frequency 1 (10 Hz) Frequency 2 (25 Hz) Frequency 3 (50 Hz)	✓	✓	✓	✓	✓	✓	✓	✓	✓	✓
4	Preload 1 (lower) Preload 2 (higher)	✓	✓	✓	✓	✓	✓	✓	✓	✓	✓
5	Short Time Period 10 Hour Time Period	✓	✓	✓	✓	✓	✓	✓	✓	✓	✓

All parameters other than those listed are not varied intentionally. These non-varying parameters include temperature, oil viscosity, and pressure drop across the seal (to be held at zero).

Figure 2 Test Matrix

test, a time duration -- 10 hours rather than several minutes -- is specified.

The test matrix does not include consideration of several other parameters. These include temperature, oil viscosity, and pressure drop across the seal. These parameters are not varied intentionally for the test program. The temperature was approximately room temperature. The oil was Mobil XRL-1032 AR-1. The pressure drop was essentially zero; i.e., that produced by the level of oil above the seal.

Measurement Techniques

This section discusses the techniques used in measuring leakage, seal friction force, and oil film thickness.

Leakage and Force Cell Calibration

For the most general test condition of Figure 2, three measurements are made. These measurements are for leakage, friction force, and oil film thickness distribution. Of these, the measurement of leakage is the most straightforward. In this, the oil level above the seal is measured before running. After a known period of operation at a measured frequency, the apparatus is stopped and the oil level is measured again. The level change gives the oil leakage directly -- calibration of this level change is via a 2×10^{-6} m^3 syringe. The leakage is then expressed in terms of average m^3 per cycle.

Measurement of the friction force is less straightforward. The experimental apparatus does contain a load cell (see page 15 of [4]). However, to obtain accurate measurements, this load cell must be calibrated carefully. Such calibration is difficult because the cell is of the piezoelectric type -- it can indicate only non-constant forces that vary at frequencies of at least several Hz. As a result, the task of obtaining an accurate measurement of the friction force at the seal/cylinder becomes, in large part, the problem of producing a dynamic force cell calibration.

To calibrate the load cell for the typical 10 Hz frequencies being employed, the following technique was used: The plunger (see page 15 of [4]) was removed from the stationary plate and mounted on the shaft. The shaft was then run at 10 Hz and the output voltage of the force cell was noted. A known trial weight (mass approximately 0.85 kg) was added to the plunger at the test seal location. The shaft was again run at 10 Hz and the new force cell voltage output was noted. With these measurements, the sensitivity of the force cell, including all associated electronics and plunger mounting

compliance effects, was obtained from the formula

$$\text{Force cell sensitivity (V/N)} = \frac{\text{volts with trial weight - volts without trial weight}}{\text{mass of trial weight x acceleration}}$$

in which the mass of the trial weight is in kg, and the acceleration is in $m \cdot s^{-2}$. All measurements were taken for peak values, so that the acceleration, for the known frequency and displacement, is

$$\text{acceleration} = (1/2) \cdot (\text{stroke}) \cdot (\text{frequency})^2$$
$$= (0.5) \cdot (0.0254) \cdot (2\pi \cdot 10)^2 = 50.14 \ m \cdot s^{-2}$$

The calibrated sensitivity of the load cell was found to be 0.14 mV/N. This sensitivity is sufficient to resolve readily friction forces on the order of 0.7N (0.15 lbs.).

It was found that this calibration procedure, which relies primarily on the smooth and consistant behavior of the test apparatus, was both repeatable and accurate. From the precision of the voltage, mass, and frequency measurements, it is estimated that calibration accuracy to the 10% level was achieved (i.e., the friction force is measured to within 10% of its true value).

Measurement of the film thickness between the seal and cylinder is significantly more difficult than the measurement of leakage or friction force. The technique developed for this film thickness measurement is described below.

Oil Film Thickness Distribution

Measurement of the oil film thickness between the seal and cylinder is the focal point of the experimental work. It is this measurement that provides the most sensitive basis for analytical/experimental comparison and for understanding of seal behavior.

In the Interim Report [4] the discussion of measurement techniques concluded that optical interferometry is the most appropriate means of providing this important measurement. The discussion also covered the general requirements for producing the necessary interference fringes in the seal/cylinder contact region.

It was the goal of much of the work during the program to convert these general requirements into an operating procedure. The description of the resulting operating procedure is facilitated by a review of the optical interferometry technique. In brief, the technique requires that light be directed at the oil film in the seal/cylinder contact zone. The reflected light is photographed. This reflected light is composed of two parts: the beam from the cylinder-oil interface and

the beam from the oil-coated rubber interface. At certain oil film thicknesses, these beams will cancel one another. The photograph will show these cancellations as a set of bands. The oil film thickness along each band is constant and the oil film thickness change between the two adjacent bands is also constant. The photograph therefore gives the oil film distribution in the contact zone; however, the absolute thickness of the oil film is not given.

The absolute thickness of the oil film at at least one point in the contact zone is needed in order to fix the film thickness distribution. (Once the film thickness at this point is known, the film thickness at another point can be found from the photograph). However, establishing this absolute thickness is difficult for the case of the reciprocating elastomeric seal. The difficulty occurs because the film thickness varies cyclically. The cyclic variation produces a non-monotonic increase in film thickness with time even though the cyclic frequency is increased gradually to its steady state value. Therefore, the common technique of counting fringes "born" is nearly useless, unless many photographs are taken to track the complete development of the oil film from at-rest. This is difficult to do, especially since an intense flash must be used to obtain a photograph and since recharge times for flash units can be large (on the order of tenths of seconds).

To avoid the difficulties of the "fringes-born" approach, another technique for determining the absolute oil film thickness was employed. This technique used two, rather than one wavelength of light. Each wavelength produces its own black-and-white interference photograph. The shift of the band pattern between the two photographs implies the absolute film thickness. The relationship between the band pattern shift and the absolute film thickness is described in Figure 3.

Figure 3 shows a magnified cross-sectional view of the seal/cylinder contact zone. With an incident light beam of a given frequency, the dark (interference) bands would appear at points indicated by the solid dots. If the frequency of the incident light is increased (i.e., the wavelength is smaller), the location of the dark bands shift. Such a shift is indicated by the open circles. At specific values of film thickness, such as the one denoted by A, no shift would be discernible. The apparent lack of a band shift at this point occurs because an integral number of fringes between the transparent cylinder-oil interface and point A are produced for either of the two light frequencies used. In other words, while for the first frequency N fringes occur between the cylinder-oil interface and point A, for the second frequency N+1 (or N+2, N+3, ...) fringes occur. In a photograph taken with either light frequency, a dark band or fringe would occur at all points such as A. The use of these points, termed points of fringe overlap, is central to the inference of the absolute oil film thickness.

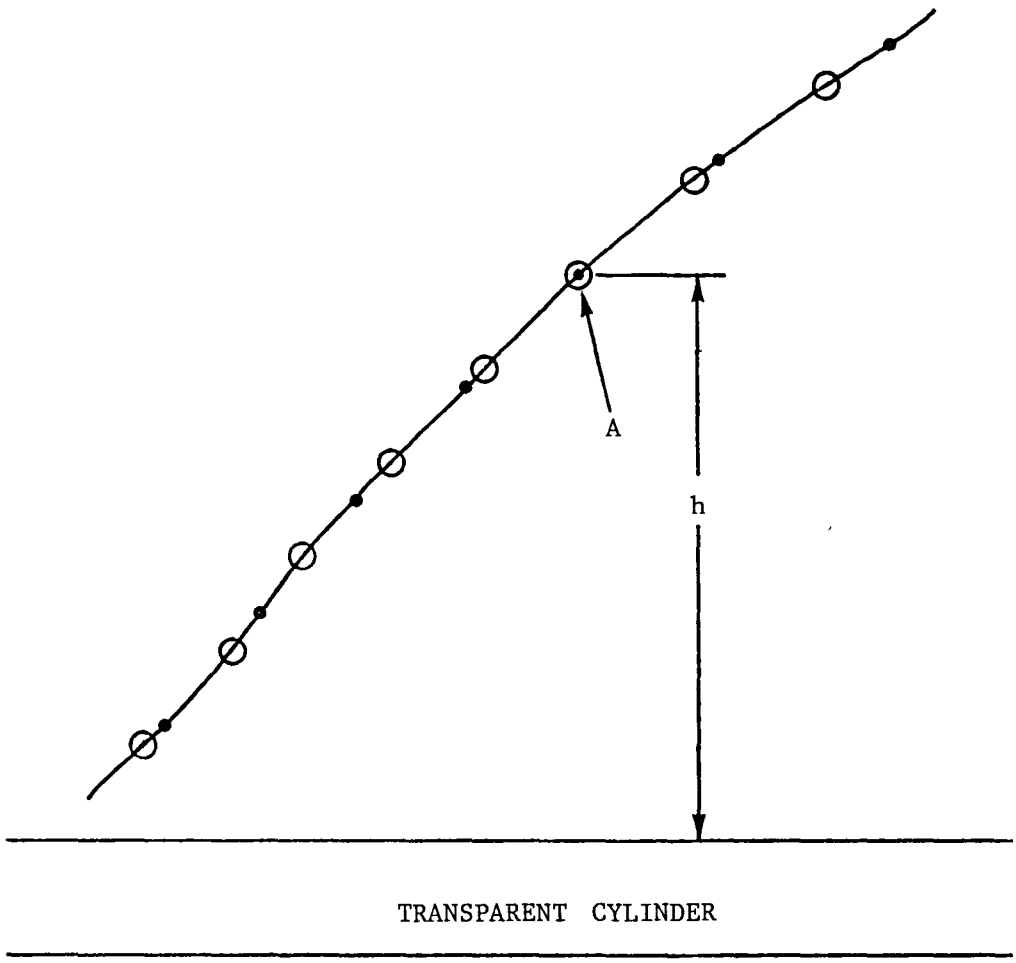

Figure 3 Fringes Produced by Two Distinct Wavelengths of Light

Referring again to Figure 3, the Nth fringe for light of the first wavelength is related to the absolute standoff (film thickness) at A by the relationship

$$h = N_1\lambda_1/2$$

where λ_1 is the wavelength in oil of the first light frequency. In this relationship, the incident light is taken to be normal to the surface of the cylinder. Also, at the fringe overlap point A, the N+i fringe for the second light wavelength occurs. Consequently, one can write

$$h = (N_1+i)\lambda_2/2$$

Elimination of N_1 between these two equations gives

$$h = \frac{i}{2} \cdot \left(\frac{\lambda_1\lambda_2}{\lambda_1-\lambda_2} \right) \qquad (1)$$

This relationship shows that, at a fringe overlap point in the photograph, the absolute film thickness can be calculated, providing that the wavelength for each light frequency is known and that the value of i is known. The value of i, which indicates that the ith overlap occurs at the fringe overlap point, is not known from the two photographs. However, its value (typically 1) can be established indirectly by taking several sets of two photographs (see section on Experimental Results).

Although Equation (1) can be used to establish the absolute oil film thickness, it must be modified for the conditions in the experimental apparatus. One modification of the apparatus is due to the incident light being not normal to the surface of the cylinder. The non-normal incidence has the benefit that the microscope need not view the glare from the front surface of the cylinder. However, this non-normal incidence complicates Equation (1) somewhat. Another modification for the apparatus is that the light wavelength is known in air from the properties of the optical filter. However, Equation (1) requires the wavelength be that in oil. The final modification is produced by the procedure used for determining the absolute oil film thickness. This procedure involves the use of several sets of photographs. However, if several filters are available, the number of light wavelength combinations can become large. Since each combination for light wavelengths can produce a different value in (1), many evaluations of the fringe overlap formula must be made.

The above considerations suggest that a simple computer program be written to evaluate h for various combinations of the two light wavelengths λ_1 and λ_2. Such a computer program was prepared (in BASIC)

and is given in Appendix A. The program uses the light incidence angle (approximately 30° from the normal to the cylinder), the index of refraction of the oil (1.4605), and the wavelengths of the available filters (0.45, 0.50, 0.55, 0.60, and 0.65 μm) to compute h for the first fringe overlap (i = 1). The program also computes, for each light frequency, the change in oil film thickness per dark fringe that occurs in the contact zone. The results of the program are given in Figure 4.

The figure shows the distance h to the first (i = 1) fringe overlap plotted against the difference between filter wavelengths $(\lambda_1-\lambda_2)$. The 4 curves are for various values of the base filter wavelength; i.e., the filter wavelength that is the smaller of the two filters being used. For example, if an orange and blue filter combination were being used, the base filter wavelength would be 0.45 μm (blue). Also, value for the horizontal axis would be 0.60-0.45 = 0.15 μm. All combinations of the available filter wavelengths are shown on the plot.

The plot indicates that the first fringe overlap can occur at an oil film thickness from 0.47 μm (18.5 μin.) to 2.5 μm (98.4 μin.). This is a large span, and is very well suited to the oil film thickness expected in the experimental apparatus. The plot also shows the sensitivity of the optical procedure in terms of oil film thickness change per observed fringe line. This sensitivity ranges from 0.144 μm (5.68 μin.) per fringe with the blue filter to 0.208 μm (8.20 μin.) per fringe with the red filter. These sensitivities also are well suited to the expected variations in oil film thickness for the elastomeric seal.

Testing Technique and Conditions

The two-wavelength procedure for measuring the oil film thickness is implemented by using the following approach:

1. The photographic flash, provided by a 35 mm camera flash attachment, is synchronized with the cylinder position. This synchronization is obtained by triggering the flash with the optical shaft encoder described earlier in this report.
2. The light from the flash is directed at the contact zone by means of the rectangular acrylic plate as shown in Figure 5.
3. The light reflected from the seal/cylinder interface is viewed with a stereo microscope. Attached to the object end of the microscope are two narrow band pass optical filters. The filters are placed so that one wavelength of light enters one side of the

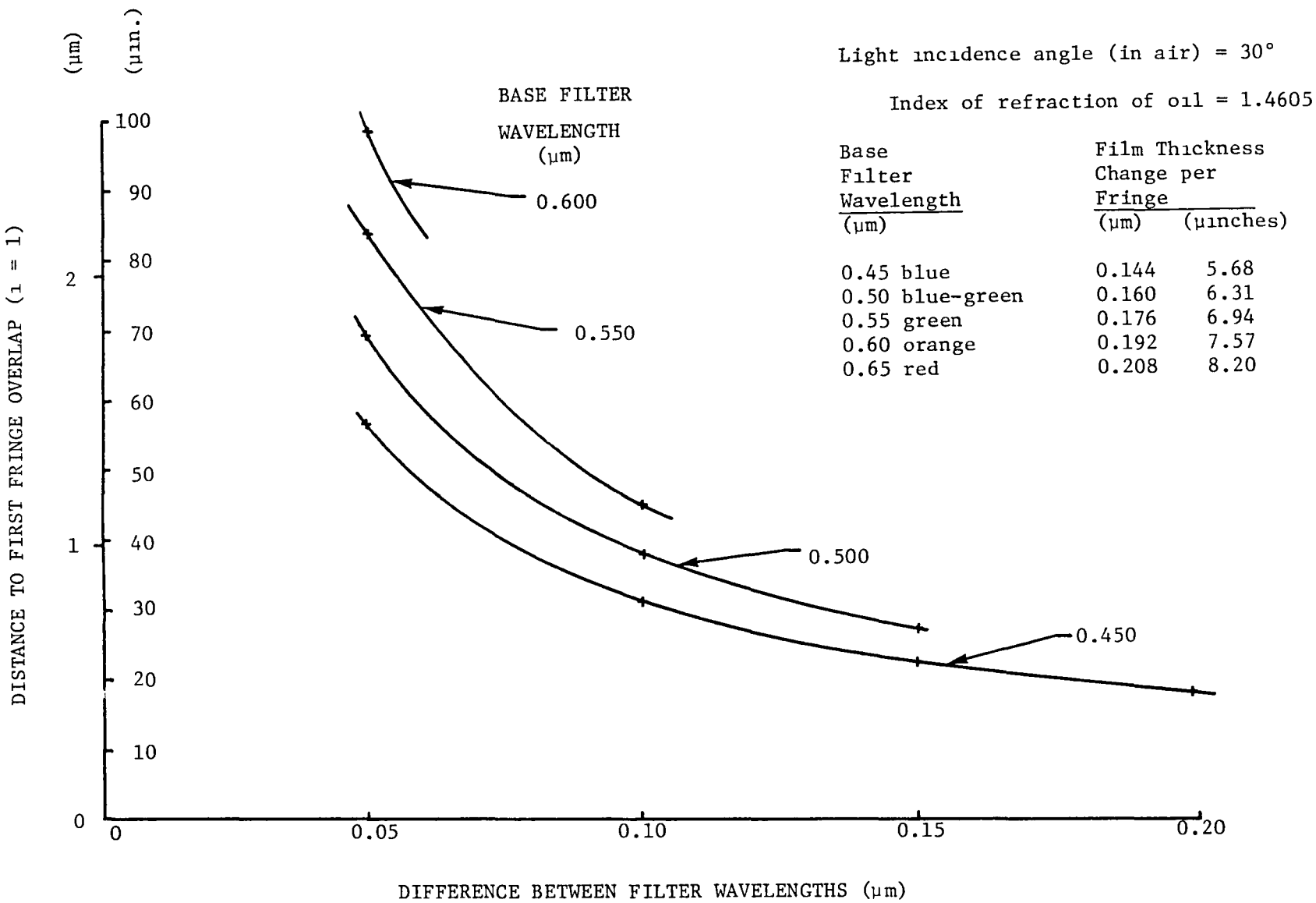

Figure 4 Characteristics of Two-Wavelength Fringe Overlap

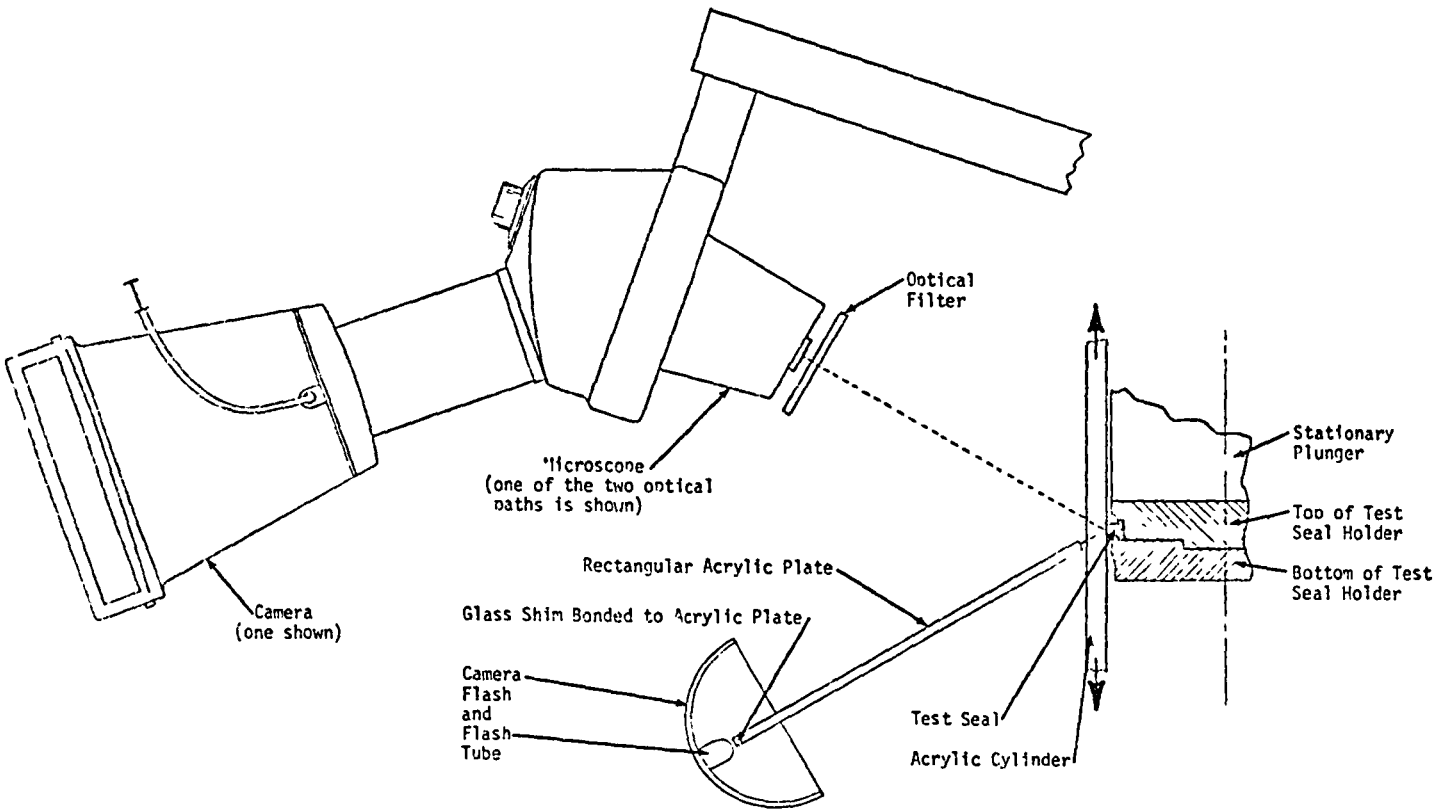

Figure 5 Schematic of Optical Setup

microscope and the other wavelength of light enters the other side of the microscope.

4. An instant-developing camera is attached to each eyepiece. Each camera is loaded with black-and-white film but is exposed by only one of the two wavelengths of light.
5. The experimental apparatus is turned on, after which the shutters of both cameras are opened. The synchronized flash is activated so that between 8 and 20 exposures are produced on each film. The shutters of the cameras are then closed. The developed photographs are used to determine the oil film thickness (see the Experimental Results section).

Producing good quality photographs requires that attention be paid to a number of practical details. These details are summarized below:

Acrylic Cylinder

The acrylic cylinders scratch easily and can craze if a solvent such as acetone is used to clean them. Photographic results are enhanced if a polishing procedure involving successively fine grit size is employed. An acceptable procedure is to apply by hand a compound containing, 1, 0.3, and 0.005 μm particles. The ends of the cylinders should have the I.D. edge smooth and rounded to facilitate entry of the seal and to minimize scratching of the coating on the seal.

Coating of Seals

Several types of coatings were tested. These include enamel, acrylic, synthol, and lacquer. The lacquer coating was found to be the most satisfactory in terms of adhesion, flexibility, durability, and quality of the interference fringes. The requirements for interferometry necessitate the use of a black coating (a white coating tends to produce too much reflectance from the oil-seal interface and thereby tends to "wash-out" the fringe pattern -- see [4]). The coating should be applied to a smooth elastomeric surface -- this can be obtained by sanding the seal with crocus cloth. A dipping process is most satisfactory for coating, and a clean environment is important. The properly-dried coating must be polished following the procedure described for the acrylic cylinder.

Seal Installation

The seal must not be scratched or stretched during installation on the test seal holder. The nylon backing rings for the "T"

seal cannot be used because they scratch the acrylic cylinder. (The two part seal holder avoids the need for seal stretching during installation and also produces the axial support to the seal otherwise provided by the backing rings.) The seal and acrylic cylinder should be coated with oil during the installation of the plunger to minimize scratching of the seal coating.

Light Source

The light source used should have a straight flash tube -- this flash tube must be placed against the glass shim on the end of the rectangular acrylic plate (the front cover of the flash unit must be removed). The angle (incidence angle) of this place with respect to the normal to the surface of the acrylic cylinder should be as small as possible; however, the front surface reflection (glare) from the acrylic cylinder limits this angle (a 30° incidence angle was found to be satisfactory).

Microscope and Cameras

The microscope should be positioned so that the viewing angle with respect to the normal to the surface of the acrylic cylinder is equal to the incidence angle. Eyepieces should be retained in the microscope when the cameras are installed -- this gives a large field of view on the photographs. Care must be taken to align the optical system such that part of the area photographed by one camera also appears in the other photograph. Also, care must be taken to insure that the flash illuminates properly the seal area being photographed. Vibration of the plunger and camera support system must be minimized to avoid blurred photographs.

A procedure was followed during testing to avoid neglecting any of the above details and to prevent disregarding other important aspects of rig operation. This procedure is outlined in Appendix B.

Experimental Results and Discussion

This section presents and discusses results that were obtained from the experimental apparatus. These results do not represent an in-depth investigation of the behavior of an elastomeric seal; rather, the results indicate the types of measurements that can be made and constitute a first attempt at experimental-analytical comparison. The results also give some indication of the effects on seal behavior when a limited number of seal-related and cylinder-related parameters are varied.

The section first gives the friction force and leakage results ob-

tained. The section then covers the 3.6×10^4 s (10 hour) test. After that the photographic data for oil film thickness are given and determinations of film thickness distributions are made. The end of the section covers experimental-analytical comparisons and the discussion of the data.

Friction Force and Leakage

Tests were run according to the Test Matrix given in the preceding section. The tests complied with that test matrix as closely as possible; however, in one case, an exception to the test matrix had to be made. This exception concerns the oscillation frequency. The desired frequency of 50 Hz had to be avoided because of a rig resonance. For this reason, a 45.5 Hz frequency was used.

The results of the tests were given in Table 1. In the table, the tests (columns) of the Test Matrix are denoted by the T.M. No. (i.e., by the rows of Table 1). The columns of Table 1 give both information regarding the testing conditions and results obtained from the tests. The second column from the left indicates the type of seal used in the test. The symbol "T" in the column denotes the T seal while the "O" denotes the O ring. The third column denotes the durometer of the elastomer. This elastomer is hard (90 durometer) or soft (70 durometer). The fourth column indicates whether a shim was used under the seal to increase the preload. The fifth column shows whether the backing rings were used. The sixth column concludes the seal information by indicating the presence and extent of coating on the seal. When present, the coating was either partial (about 30° of the circumference of the seal) of full (completely around the seal). In either case, the coating was applied to the seal so that, in the plane through the cross-section of the seal, the coating extended well beyond the contact zone (but not to the "T" portion of the seal).

The next column of the results table refers to the cylinder used. The cylinder was either acrylic or aluminum. For the acrylic cylinder, unpolished denotes that the I.D. was in the as-received condition. Polished denotes that the polishing procedure of the previous section was used. For the aluminum cylinder, finish I denotes an as-machined surface finish (roughness approximately 0.4 μm rms (16μ in. rms)). Finish II denotes the application of polishing procedure of the previous section to the aluminum cylinder. The result of that polishing procedure was a roughness of approximately 0.1 μm rms (4 μin. rms).

Test results are given in the next 3 columns. The first column denotes the measured preload at the static (not sliding) condition. This preload is given in terms of the ratio of measured axial contact

TABLE 1

FRICTION FORCE AND LEAKAGE RESULTS

T.M. No.	SEAL INFORMATION					Cylinder	Preload	Peak Force (N)	Peak Force (lbs.)	Leakage (10^{-10} m^3/cy)
	Type	Durometer	Shim	Backing Rings	Finish					
1	T	Hard	No	No	Fully Coated	Polished	0.520	28.1	6.32	1.67
2	T	Soft	No	No	Part. Coated	Polished	$\bar{\mu}$=0.547 σ=0.044 n=5	$\bar{\mu}$=17.1 σ=0.80 n=5	$\bar{\mu}$=3.85 σ=0.18	$\bar{\mu}$=4.67 σ=1.92 n=5
3	0	Soft	No	No	Part. Coated	Polished	$\bar{\mu}$=0.448 σ=0.166 n=3	$\bar{\mu}$=16.2 σ=7.43 n=3	$\bar{\mu}$=3.63 σ=1.67	$\bar{\mu}$=11.68 σ=4.42 n=3
4	T	Soft	No	No	Part. Coated	Unpolished	0.428	10.7	2.40	46.7
5*	T	Soft	No	No	Part. Coated	Unpolished	0.428	3.5	0.79	Unknown
6	T	Soft	7.6×10^{-3} mm (0.3 mil)	No	Fully Coated	Polished	0.726	19.0	4.26	4.2
7	T	Soft	No	No	Uncoated	Polished	$\bar{\mu}$=0.561 σ=0.048 n=3	$\bar{\mu}$=17.7 σ=1.93 n=3	$\bar{\mu}$=3.97 σ=0.435	$\bar{\mu}$=5.06 σ=2.89 n=3
8	T	Soft	No	Yes	Uncoated	Alum., Finish I	**	20.4	4.58	0.83
9	T	Soft	No	Yes	Uncoated	Alum., Finish II	**	20.0	4.50	1.67
10	T	Soft	No	No	Uncoated	Unpolished	0.533	$\bar{\mu}$=14.7 σ=4.3 n=28	$\bar{\mu}$=3.31 σ=0.97	$\bar{\mu}$=2.96 σ=0.97 n=7

*Frequency = 45 Hz

**Unable to Measure

length to the cross-sectional diameter of the seal. This contact length was measured by viewing the contact zone through the microscope and comparing the axial length to the known axial seal groove length.

For the preload, as well as for the last two columns, either a single entry or 3 entries are given for a particular test. A single entry denotes that one measurement was made of the indicated quantity. The three entries denote that more than one measurement was made of the quantity. For tests in which more than one measurement was made, the number of measurement is given by n. The average of the n measurement is denoted by $\bar{\mu}$. The quantity σ gives the standard deviation of the n measurements.

The next-to-last column gives the measured force. The value given is the peak value of the essentially sinusoidal force variation with time. An example of the force data, obtained via a low pass filter*, is given in Figure 6. The figure is a photograph taken of the oscilloscope screen for one of the tests constituting T.M. No. 4. For the figure, the horizontal scale is time. Each large division is 20 ms, so that the frequency shown in about 17 Hz. The vertical axis denotes force, with each division being 1mV per large division. Since the sensitivity of the force cell is 0.14mV/N, the peak (one half of peak-to-peak) force given by the photograph is approximately 11.5N (2.6 pounds).

The photograph indicates why only one value (the peak value) for the force measurement is given in Table 1. It was found that for a given test, the sinusoidal behavior of the force did not change measurably with time. Even in the 10 hour test, only a 2% variation from the start of the test to the end of the test was observed in the value of the peak force.

The last column of Table 1 lists the measured leakage for the tests. This leakage occurs with essentially no pressure drop across the seal --

*The corner frequency of the filter was set at 25 Hz.

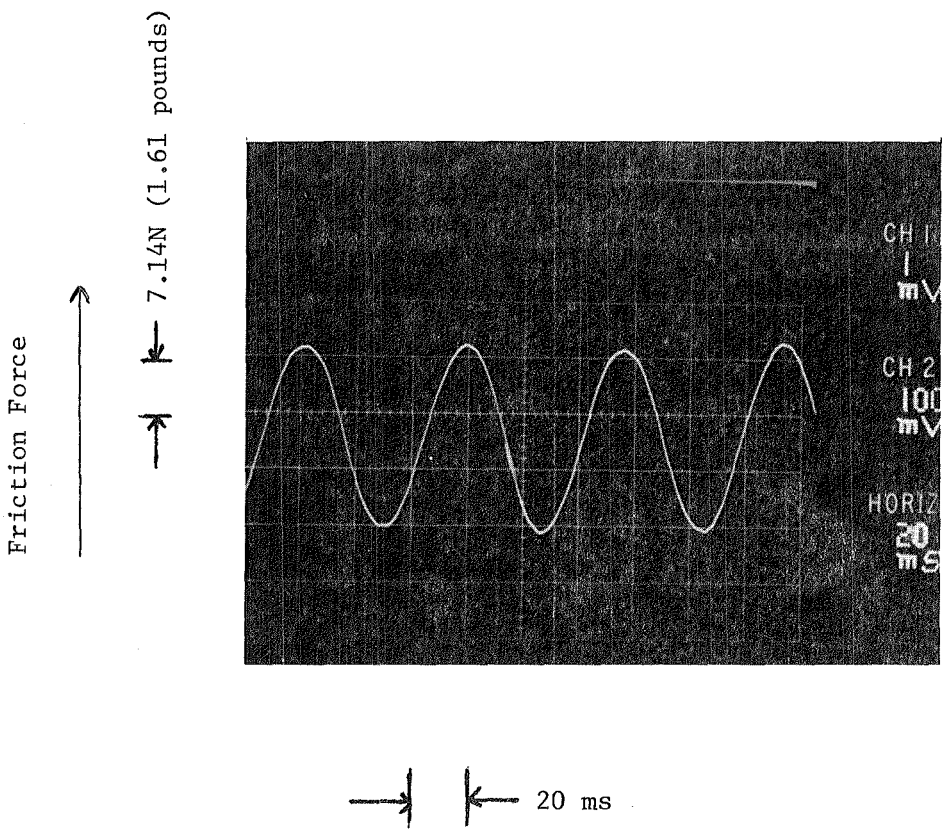

Figure 6 Friction Force Versus Time
For T.M. No. 4

the only net pressure is that due to approximately 25 mm (1 in.) of oil head above the seal. The leakage listed is given on a per cycle basis, although the measurements were made on a several minute (several thousand cycle) basis.

Ten Hour Test

The results obtained for the 3.6×10^4s (10 hour) test (T.M. No. 10) have been summarized in Table 1. However, because data were taken throughout this test, a more detailed presentation of the data is warranted.

Results from the ten hour test are given in Figure 7. The figure shows, plotted vs time, two temperatures, the peak force, and the oil leakage rate. The first thermocouple (T.C. 1) is that above the seal -- it protrudes slightly into the oil film. The second thermocouple is just behind the seal in the aluminum test seal holder. The leakage rate is shown on a per cycle basis -- it was computed on the basis of total oil leaked after start of the test divided by total cycles since start of the test. As a result, the leakage figures become more of a test average as more cycles are included in the running total.

A few points regarding the test and the figure are of interest. The thermocouples show a rising temperature trend for the first two hours. The rather abrupt decrease at that time was due to the start of water cooling. Also, the force can be seen to be very constant throughout the test. This occurred even though the test was stopped (approximately once per hour) to check oil leakage and to add oil.

Film Thickness Data

Optical interference photographs were sought for Test Matrix tests number 1 - 6. As indicated earlier, to infer the absolute oil film thickness several sets of photographs can be required. Each set of photographs is produced by one filter combination and, consequently, defines a different value of absolute oil film thickness at which the first fringe overlap occurs.

For the Test Matrix test number 1, such sets of photographs were obtained. One of these sets of photographs is shown in Figure 8. Also shown in Figure 8 are the conditions under which these photographs were taken. The left photograph was exposed with 0.55 μm (green) light using 12 flashes. The right photograph was exposed with 0.600 μm (orange) light using 7 exposures.

The photographs show approximately 3 mm (1/8 in.) of the circumferential contact periphery. In the photographs, this circumferential direction is horizontal. The vertical direction in Figure 8 corresponds to the axial direction for the seal. The leading edge is at the top of the photograph so that, in the apparatus, the cylinder was moving down at the instant the flashes occurred.

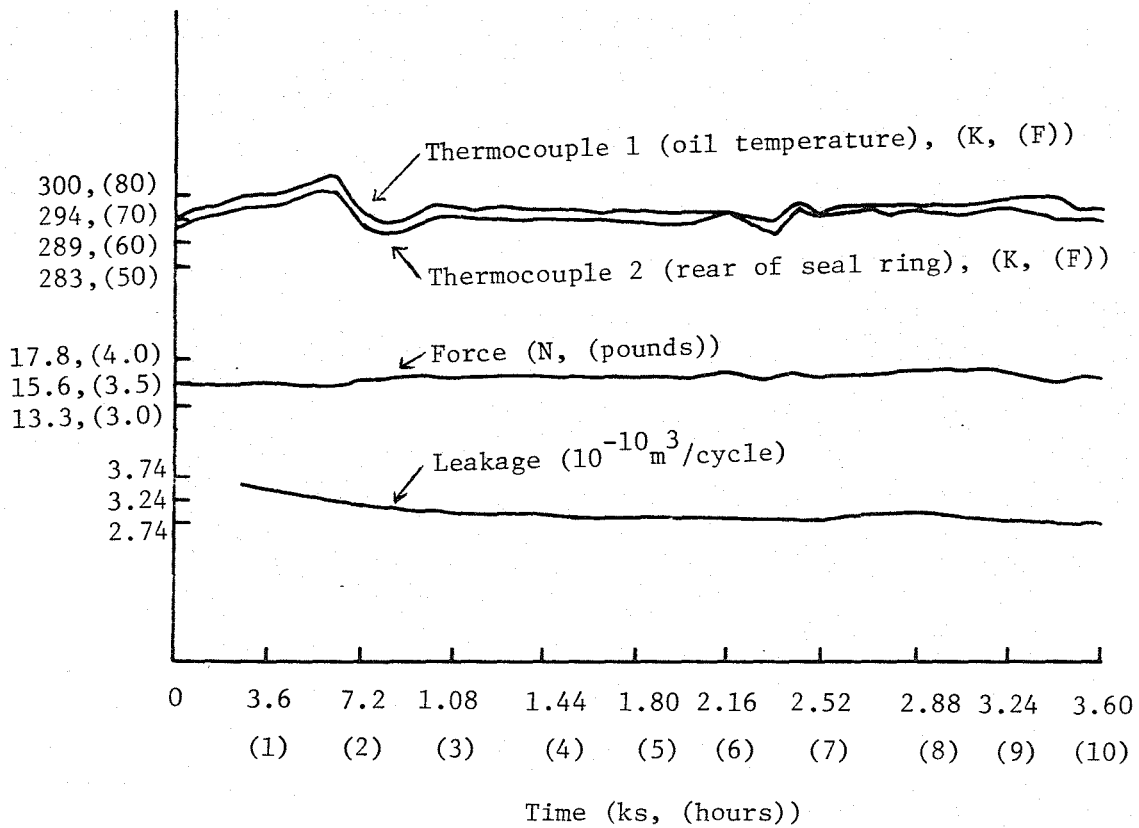

Figure 7 Results of the Ten Hour Test

Figure 8

Interferometric Results

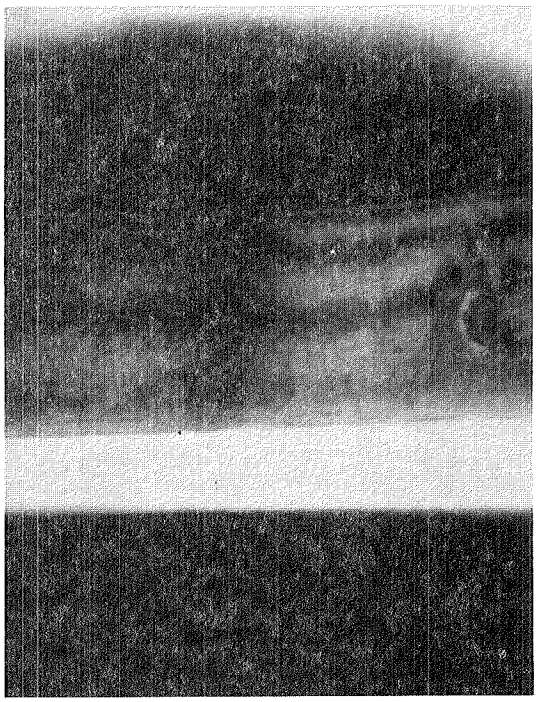

GREEN FILTER (0.550 μm)
12 EXPOSURES

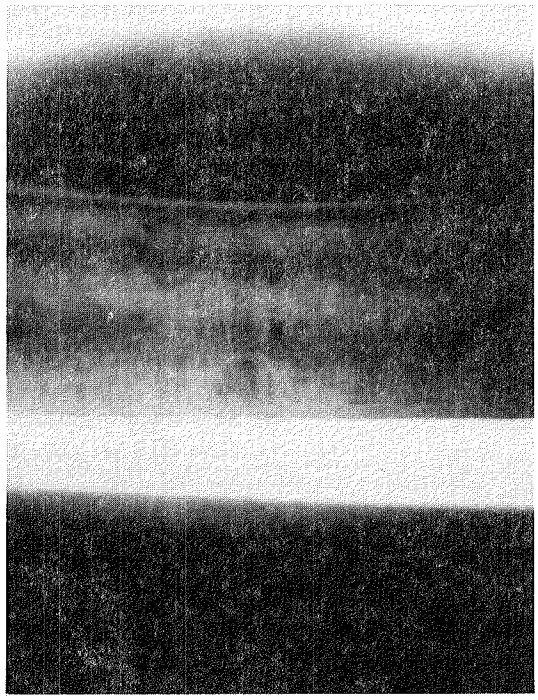

ORANGE FILTER (0.600 μm)
7 EXPOSURES

CONDITIONS

Seal: hard T seal (90 durometer)

Preload: 52%

Frequency: 10 Hz

Cyclic Position: 30° before top dead center (cylinder on downward stroke)

Applied Gas Pressure: 0 Pa (0 psi)

Force: 28.1N (6.32 pounds) peak

Leakage: 1.67×10^{-10} m^3/cycle

The contact zone in the photographs extends over the axial length denoted by the arrows. In this contact zone, several dark fringes occur. Because these fringes are distinct, and because approximately 1800 cylinder cycles* occurred during the photographic process, one can conclude that the fringe pattern is quite deterministic (as opposed to random). This, due in part to the smoothness and rigidity of the experimental apparatus, is quite fortunate -- only with multiple exposures would sufficient light be delivered to the photograph for adequate exposure.

The photographs show that for the particular set of test conditions used the film thickness is essentially axisymmetric. This axisymmetric behavior is indicated by the fringe bands which are perpendicular to the axial direction. The photographs also show that some local irregularities exist in the film profile. One such irregularity can be seen in the right photograph at the center of the trailing edge. The same irregularity also can be seen in the left photograph. These irregularities can be caused by particles imbedded in the seal and by cracks or breaks in the coating on the seal. The presence of such irregularities is desirable unless their presence affects the overall film thickness distribution being photographed. The irregularities serve as reference points for use of the photographs in determining the oil film thickness (see the following section).

It can be noticed, particularly in the center of the left photograph, that the circumferential fringe pattern disappears. This disappearance is caused by nonuniformity in the lighting conditions. The nonuniformity is different for the two photographs because optical paths for the two objective lenses of the microscope are not coindicent -- these paths are several degrees apart in the circumferential direction of the seal.

Another set of photographs is given in Figure 9. The only condition that differs between this set and those of Figure 8 is the seal type -- for Figure 9 the soft (70 durometer) rather than the hard (90 durometer) seal was used. Consequently, Figure 9 is for Test Matrix number 2.

The optical interference fringes can also be seen in this set of photographs. However, in comparison to those of Figure 8, the fringes are less regular. More circumferential variations in the fringes occur. In addition, the axial fringe spacing is different when compared to the spacing in Figure 8. This indicates that the oil film thickness distribution is not the same for the hard and for the soft seal. This difference is considered in detail in the following section.

Irregularities in the fringe pattern also occur for the softer seal. In contrast to the irregularities in Figure 8, those in Figure 9 are bright dots. These bright dots may have been caused by broken small

*10 Hz times 60 seconds per minute times (approximately) 0.25 minutes per exposure times 12 exposures.

Figure 9

Interferometric Results

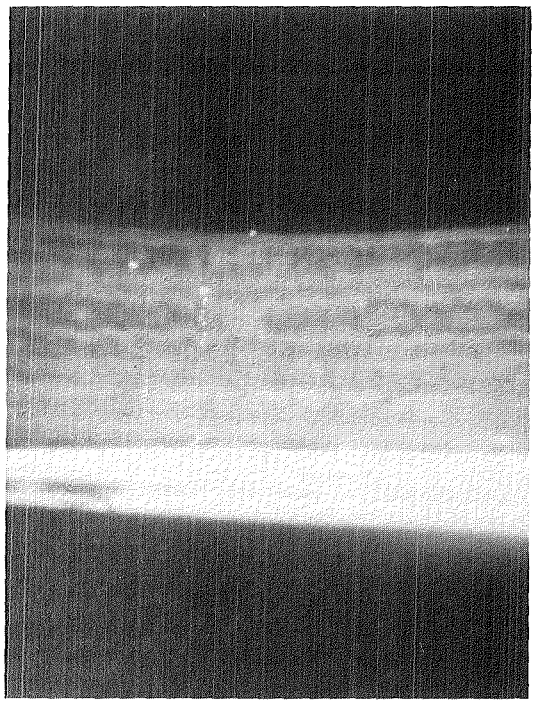

GREEN FILTER (0.550 μm)
16 EXPOSURES

ORANGE FILTER (0.600 μm)
10 EXPOSURES

CONDITIONS

Seal: soft T seal (70 durometer)

Preload: 49%

Frequency: 10 Hz

Cyclic Position: 30° before top dead center (cylinder on downward stroke)

Applied Gas Pressure: 0 Pa (0 psi)

Force: 18.3N (4.11 pounds) peak

Leakage: 1.67×10^{-10} m^3/cycle

air bubbles in the seal coating. These bubbles, when broken during polishing or during seal operation, could form small holes which could cause significant reflection of light. As in the hard seal case, these irregularities form handy reference points for measurements.

It is suspected that the majority of the difference for the two photograph sets in circumferential fringe regularity is caused by the optical coating. This coating, although carefully applied with an airbrush, varied somewhat from seal-to-seal. This variation was minimized, but not eliminated, by the polishing procedure described in the previous section. A less significant cause for the fringe irregularities in Figure 9 may be the durometer of the seal. The softer seal is the more likely to degrade both during the smoothing (sanding) operation prior to coating and during the polishing procedure itself.

In both Figures 8 and 9, a shift in the fringe pattern with the change in light frequency is apparent. In Figure 8, the change from green to orange results not only in shifting the fringes, but also in eliminating at least one fringe. In Figure 9, the shift is not as obvious; the greatest effects can be seen near the leading and trailing edges. The evaluation of this shift and the determination of the associated oil film thickness distribution is made in the following section.

Photographic results having a quality equivalent to that in Figures 8 and 9 were not obtained for T.M. Nos. 3-6. For T.M. No. 3 (the O-Ring test) and 6 (the high preload test), difficulties were encountered in producing a smooth coating on the seal. The surface obtained contained high frequency surface ripples. These ripples were of the size of the anticipated film thickness, so that the fringe patterns that appeared exhibited a random pattern. This pattern corresponded exactly to the appearance of the seals which, when removed from the rig, were studied under a microscope. The reason for the non-smooth surface was not determined -- possible sources are the coating mixture, the coating techniques, the polishing process, or the surfaces of the seals to which the coating was applied.

In the tests of T.M. Nos. 4 and 5 (the 25 and 50 Hz tests) fringe patterns could not be photographed. The photographs were blurred and suggested that the various multiple exposures had blended the fringe pattern into a relatively homogenous resultant image. It was readily apparent that rig resonances were the cause of the problem. At 25 Hz, the structure which supports the microscope and cameras vibrated significantly. Near 50 Hz, structural vibrations occurred. These vibrations caused the camera or microscope to move with respect to the seal, so that the several exposures did not produce coincident images on the film. To verify this, speed for the 25 Hz test was reduced to about 17 Hz, at which the operation of the rig was very smooth. Good quality interference photographs were obtained readily. These results suggested that freedom from vibration in the apparatus is essential in order that the multiple exposure technique be workable.

Film Thickness Distribution

The oil film thickness distribution was evaluated from the photographic results obtained for T.M. Nos. 1 and 2. This evaluation involves as its most important ingredient the determination of fringe overlap point and number (i.e., the value of i).

Review of Figure 8, which is the orange filter-green filter photograph set for the hard seal, indicates that no fringe overlap point exists. That conclusion can be reached readily by first measuring, for the center of each dark band in the right photograph, its axial distance from the irregularity at the center of the trailing edge. The same distance can then be measured in the left photograph. No correspondences in these measurements occur. This suggests that at no point in the contact zone did a film thickness of 2.1 μm (83 μin.) exist. In addition, at no point in the contact zone did a film thickness of a multiple of 2.1 μm exist.

Establishing the oil film thickness therefore requires that at least one more set of photographs be taken. Since the first fringe overlap point for the green-orange combination is 2.1 μm, and since the film thickness is unlikely to be greater than 2.1 μm, the additional set of photographs should provide the first fringe overlap point in the range, say, 0.5 - 1.3 μm (20 - 50 μin.). The blue-green/orange combination is suitable -- the first fringe overlap point for this combination is 0.96 μm (38 μin.).*

A blue-green/orange set of photographs was therefore obtained for the hard seal case (T.M. No. 1). The blue-green photograph is difficult to produce. Whereas the orange filter requires 7 flashes (exposures) and the green requires 12 flashes, the particular blue-green filter used requires upwards of 16 exposures for a workable photograph. A tradeoff in the number of flashes exists -- too few produces too dark a picture while too many can produce fringe blurring. Sixteen exposures were used for the hard seal test -- this number of flashes minimized the fringe blurring while still producing a photograph with contrast sufficient for obtaining data. However, the contrast in the photograph was not sufficient to permit reproduction for the present report. Instead of the photograph, Figure 10 gives a tracing made from the original picture. The figure also gives a tracing of the associated orange-filter photograph.**

---

*See Figure 4 and Appendix B.

**The tracing of the orange-filter photograph is given only to provide an equivalent representation. The contrast for the orange-filter photograph is sufficient for reproduction -- see Figure 8.

Figure 10 shows that a fringe overlap point seems to exist for the wide fringe closest to the trailing edge -- the distance to the center of the dark band from the trailing edge irregularity is essentially the same in either photograph. This suggests that at this fringe, the absolute oil film thickness is on the order of 0.96 μm (38 μin.) or some integer multiple of this distance. Measurement from the same irregularity to the next wide band shows that this distance is not the same in the two photographs. The next wide band therefore is not a fringe overlap point but appears to be within one fringe of that overlap point. Since the oil film thickness change is about 0.18 μm (6.9 μin.) per fringe, one can conclude that the absolute oil film thickness at the first wide band is within about 0.2 μm (7 μin.) of the 0.96 μm (38 μin.) determined above.

The above discussion does not resolve the issue of whether the oil film thickness at the fringe overlap point is 0.96 μm or some integer multiple of 0.96 μm. To resolve this, one should first determine the overall shape of the film thickness distribution. Once that shape is known, comparison of Figures 8 and 10 can be used to infer the value of i.

The shape of the film thickness can be deduced from the combination of Figure 8 and physical reasoning. In Figure 8 (right photograph) the widest band is the one nearest the trailing edge. This suggests that the most gradual slope of the film thickness distribution occurs in that region. The width of the bands and their spacing decrease as one moves toward the leading edge. Therefore, the thickness of the oil film is either increasing or decreasing from the center of the contact zone to the leading edge. The former is the more likely because no indications appear in Figure 8 to suggest an area of zero slope in this region. Such an area of zero slope would have to occur for film thickness decreasing toward the leading edge because the seal must curve away from the cylinder outside the contact zone.

The above reasoning suggests that the film thickness profile is as shown in Figure 11. The figure gives, for an assumed i=1, the oil film thickness versus distance in the contact zone. Shown on the figure are points obtained from the blue-green and from the orange filter. Also shown on the figure are the first and second fringe overlap points for this filter combination.

The question of the value of i can now be addressed. From Figure 11, the measured oil film thickness is in one of the ranges 0.97 - 1.4 μm (38 - 53 μin.), 1.93 - 2.69 μm (76 - 106 μin.), 2.9 - 4.0 μm (114 - 159 μin.), etc. as i takes on values 1, 2, 3, etc. However, the photographic results with the green/orange filter combination (Figure 8) have already precluded i having the values 2, 4, 6, etc. Physical insight, the use of simple-steady state film thickness formulas, or

Figure 10

Tracing of Interferometric Photographs

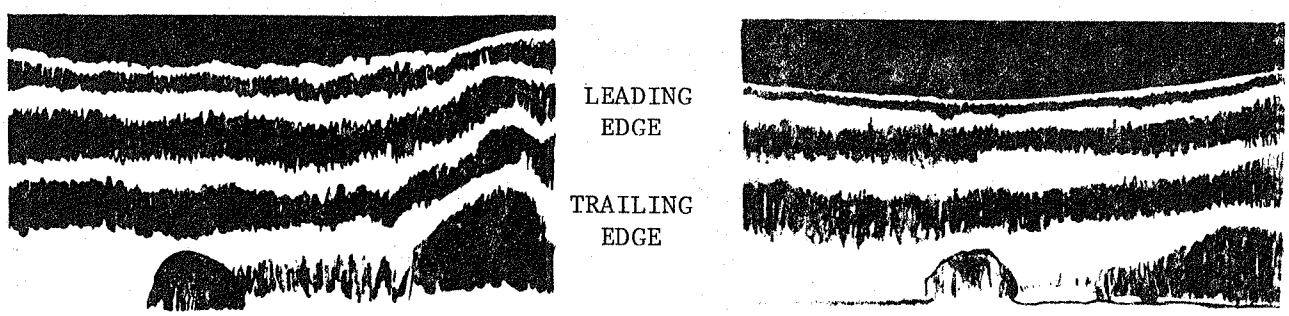

BLUE-GREEN FILTER
(0.500 μm)

ORANGE FILTER
(0.600 μm)

CONDITIONS

Seal: hard T seal (90 durometer)

Preload: 52%

Frequency: 10 Hz

Cyclic Position: 30° before top dead center
(cylinder on downward stroke)

Applied Gas Pressure: 0 Pa (0 psi)

Force: 28.1N (6.32 pounds) peak

Leakage: 1.67×10^{-10} m^3/cycle

the use of the analytical results in [4] also preclude high values of i. Consequently i = 1 or 3 is still reasonable for the results obtained. To choose between these, an additional set of photographs was taken, this time using the red-orange combination (for which, at i = 1, the fringe overlap point is at 2.50 μm (98.4 μin.). That set of photographs revealed no fringe overlap, so that this film thickness did not occur in the red/orange photograph. This information therefore eliminates i = 3 in the blue-green/orange set -- the value i = 1 appears to be the correct one.

The green filter results in Figure 8 can be used to add more points to the film thickness plot in Figure 11. To do so requires that the oil film thickness for one point in the photograph be set. This can be done readily by again employing the fringe overlap concept. Although no fringe overlap point exists for the green/orange combination, one can look in the photograph for a point where a dark band in one photograph corresponds to a light band in the other photograph. Such a point is a one-half fringe overlap point which, from Figure 4, is at about 1.1 μm (42 μin.). In the photographs, such a light band/dark band correspondence occurs at about 0.53 of the contact length.* This point in Figure 11 is shown by the open square. The solid squares give the film thickness results for the other dark bands of the green-filter photograph.

The points in Figure 11, produced by using the above analyses, provide a rather well-defined curve. This curve is shown in the figure by the solid line, and is the experimentally measured oil film thickness profile. It is to be noted that this profile is not shown near the ends of the contact zone. In those regions, fringes are difficult to distinguish. This is to be expected because the change in film thickness becomes very large as one approaches the ends of the contact zone.

A similar analysis can be made for the photographs obtained from the soft seal test (T.M. No. 2). The analysis is made more complicated for that seal because the oil film thickness is less axisymmetric than in the hard seal test. However, the results obtained from the hard seal test can be used to aid in interpreting the photographic results for the soft seal test.

The analysis employs Figure 9, in which a fringe overlap seems to exist for the dark fringe just ahead (toward the leading edge) of the center of the contact zone. Verification that this is a fringe overlap point can be obtained by comparing a measurement from a bright spot (irregularity) to the fringe in each photograph. Assuming that i = 1 and referring to Figure 4 and Appendix A, one finds that, at the fringe overlap point, the absolute oil film thickness is about 2.2 μm (83 μin.). Following the process used for the hard seal, one can measure the distance in each

*The dark band is on the green-filter photograph

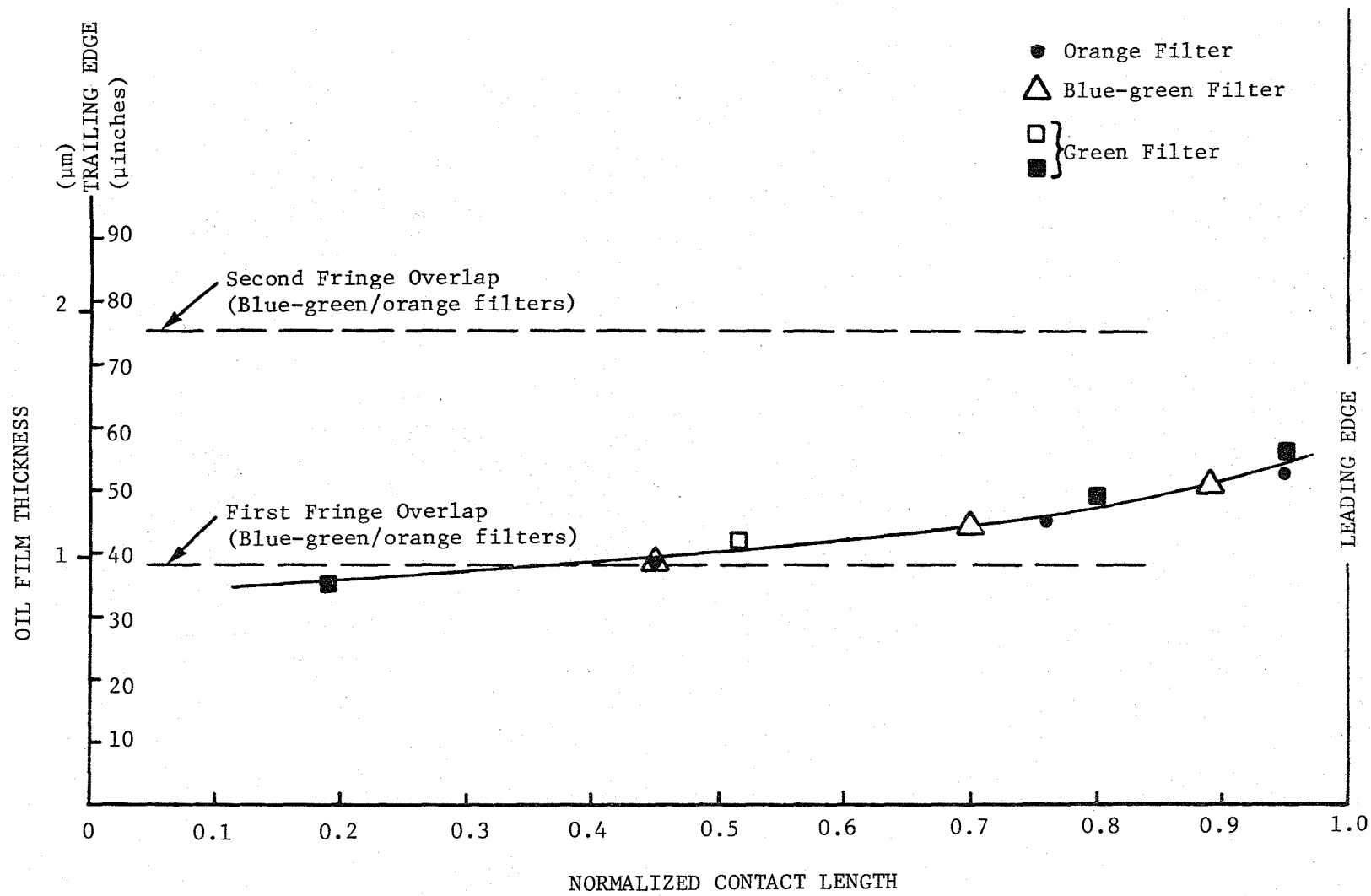

Figure 11 Experimentally Determined Oil Film Thickness (Hard Seal)

photograph from the irregularity to the next fringe (next to the overlap fringe and closer to the leading edge). Comparing the measurement indicates that this next fringe is not a fringe overlap point. Consequently, the absolute oil film thickness at the fringe overlap point is known (if i = 1) within about 0.2 μm (7 μin.) of the 2.2 μm (83 μin.) determined above.

Considering next the shape of the film thickness distribution, one can inspect the left edge of the right photograph. At this edge the general axisymmetric oil film thickness, which occurs at the center of the photograph and which was assumed in the above analysis, disappears. The light band just ahead (toward the leading edge) of the overlap fringe extends to the back (toward the trailing edge) of that fringe and to the back of the following fringe. This bright band defines everywhere a constant oil film thickness, so that in this broad rear-central region of the axial contact zone an essentially constant oil film thickness occurs. Since the forward dark band in this zone is also the fringe overlap band, this implies that the fringe just behind the overlap fringe could also be an overlap. Measurement of the distance to this next fringe from one of the bright irregularities produces the same result for each photograph. Consequently, it can be concluded that both of these fringe bands are indeed fringe overlaps and that absolute oil film thickness at these bands is about 2.2 μm (83 μin.). Also, no additional fringes occur at the rear of the contact zone. This indicates that the 2.2 μm film thickness extends well towards the trailing edge of the contact zone.

With the above information, a film thickness distribution can be plotted, Figure 12. This distribution was obtained by first plotting the fringe overlap points at 0.45 and 0.60 on the horizontal axis. Using the green-filter photograph, the points in the solid squares are located. The horizontal coordinate for these squares is located by the position in the contact of each fringe forward of the fringe overlap point. From the photograph, it is concluded that there are four such fringes, with the last two (those nearest the leading edge) almost coincident. The vertical coordinate is determined by the film thickness change per fringe for the green wavelength. Similar points result from the orange photograph. In both photographs, the second band from the fringe overlap point appears to be a single fringe and is plotted as such.

The resulting oil film thickness distribution has a behavior generally similar to that for the hard seal (Figure 10). However, the oil film thickness is much greater than for the hard seal. In fact, if i = 1 as assumed for Figure 12, then the oil film thickness for the soft seal is about twice that for the hard seal.

With the filter combinations available, one cannot determine with certainty whether the film thickness distribution in Figure 12 is

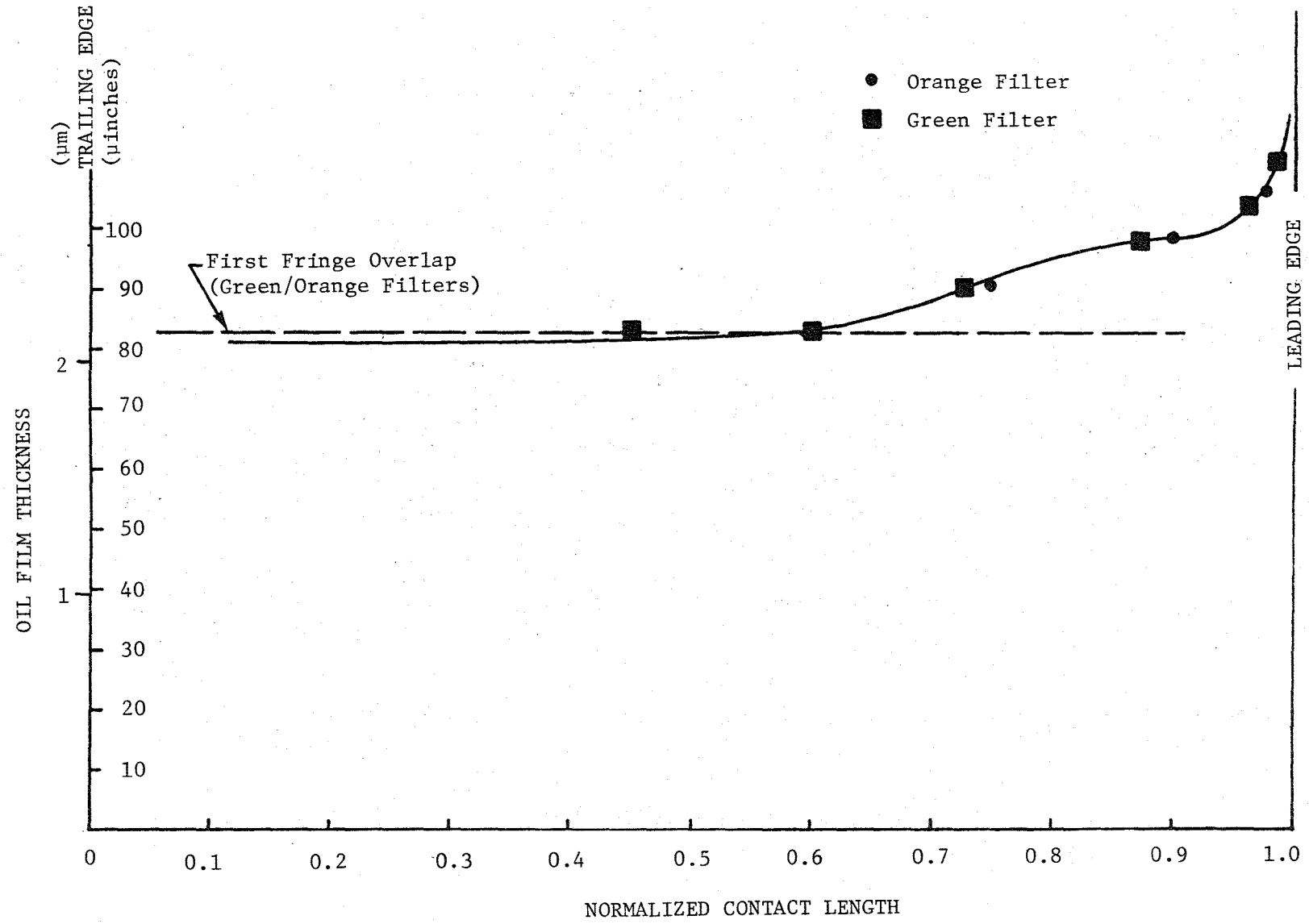

Figure 12 Experimentally Determined Oil Film Thickness (Soft Seal)

correct as shown (i.e., whether i = 1). Another set of filters can be used to provide additional information, but one is constrained by the plot in Figure 4. Using a blue/orange filter combination, the first fringe overlaps occurs at 0.577 μm (22.7 μin.). The fourth (i = 4) fringe overlap occurs at 2.31 μm (90.8 μin.). That set of photographs was taken, and did indicate a fringe overlap at about the 3/4 portion of the normalized contact length. This agrees with the results of Figure 12. The blue/orange results do not indicate the value of i for Figure 12, since when i = 8 is used for the blue/orange combination and i = 2 for the green/orange combination, the results would also agree.

The more reliable procedure for determining the value of i is to have additional sets of photographs so that the first fringe overlap point for each additional set occurs (approximately) at a multiple of the overlap point of the first set. This is the approach taken for the hard seal test described above. In this way, each of the first few multiples for the reference set can be eliminated. In the present case, the second overlap occurs at 4.23 μm (166.6 μin.) which is outside the range of the available filter combinations. All one can say from the interferometric results for the soft seal test is that the oil film thickness is no smaller than that shown; however, the thickness could be twice (or three times) that shown.

The measured seal friction can be used to verify that the correct value of i was used for the soft seal test results in Figure 12. This verification is made in the following section.

Experimental-Analytical Comparison

It is of considerable interest to compare the results obtained in the present experimental work to those from available analyses. The most relevant analysis is that in [4]. In addition, a rough comparison using the viscous shear force produced by the oil film is desirable. This rough comparison, presented first below, gives an independent check on the photographic results for oil film thickness.

The shear stress τ, associated with pure shear motion of two plates, is [14]

$$\tau = \mu \frac{du}{dy} \qquad (2)$$

in which μ is the viscosity of the fluid and du/dy is the velocity gradient across the oil film. If it is assumed, in the seal/cylinder system, that the film thickness in the contact zone is constant, then the following relations can be written:

$$\tau = \frac{F}{\pi Db}$$

$$du/dy = \frac{A\omega\cos\omega t}{h} \qquad (3)$$

where F is the viscous shear force (friction force)
D is the I.D. of the cylinder
b is the axial contact length
A is the amplitude of the oscillating cylinder motion
and ω is the oscillation frequency.

Substituting τ and du/dy from (3) into (2) and solving for F gives

$$F = \frac{\pi\mu DbA\omega\cos\omega t}{h} \qquad (4)$$

For the apparatus, and for the soft seal test, the following values are appropriate:

μ = 0.0404 Pa·s (5.86×10^{-6} lbsec/in^2) for Mobile XRL 1032-AR-1 oil at 294K (70F)
D = 76 mm (3.00 in.)
b = 2.2 mm (85 mils)
A = 13 mm (0.50 in.)
$\omega = 10 \cdot 2\pi = 62.8$ rad·s^{-1}
$\omega\tau = \pi/3$*
h = 2 μm (80 μin.)

Substitution of these values into (4) gives F = 4.1N (0.92 pounds). This force is below the 16.5 - 17.8 (3.7 - 4.0 pound) range (± 1σ) listed for the soft seal (T.M. No. 2) in Table 1. However, the value given in that table is the peak measured force. At the 30° before top dead center position, the velocity is half that at maximum sliding, and the film thickness (from [4], run 53) can be 16% greater than at maximum sliding. Consequently, the measured force in Table 1 corresponds to a measurement of 7.1 - 7.6N (1.6 - 1.7 pounds) at the 30° BTDC cycle point. This is approximately 44% greater than that computed from Equation 4.

* The thickness 2 μm was measured at 30° before top dead center of the cyclic motion. Consequently, $\omega\tau$ takes the corresponding value of $\pi/3$ rad.

For the hard seal test (T.M. No. 1) all values for Equation (4) are, with the following exceptions, the same as those for the soft seal test (T.M. No. 2):

$b = 2.1$ mm (81 mils)
$h = 1$ μm (40 μin.), approximately.

With these values, Equation (4) gives 7.8N (1.6 pounds). The measured friction-force for the hard seal test is 28.1N (6.32 pounds). When corrected for instantaneous cyclic speed and cyclic film thickness variation, the measured force corresponds to a measurement of $0.5 \times \frac{1}{1.16} \times 28.1 = 12.1$N (2.72 pounds). This is 41% greater than that computed from Equation (4).

Comparison of the experimental results with the analytical results in [4] is of considerable interest. To produce this comparison, it is necessary to have experimental values for several analytical parameters and to run the computer program with these values.

For the T seals used, the value of E (Young's modulus) is the most difficult to obtain. Reliable values of E are not tabulated for the fluroelastomer used and are not available from seal manufacturers. As a result, the value of E had to be measured directly. The following two techniques were used:

In the first measurement, a several-inch piece was cut from the seal and stretched. The value of E was computed from the measured strain and from the known applied force. The cross-sectional area was computed from appropriate measurements.

In the second measurement, a short piece of T seal was placed under an optical flat and loaded by a known weight. The contact footprint was measured optically. The value of E was computed using the line-contact Hertzian formula [15].

The results of both measurements indicated that the value of E for the soft seal is in the neighborhood of 4.34×10^3 kPa (630 pounds/in.^{2}). The value of E for the hard seal is approximately twice that for the soft seal.

With the value of E available, the non-dimensional parameters in [4] can be calculated. These non-dimensional parameters are p_o/E, S/R, and U, where

p_o is the pressure at the axial center of the contact zone.
S is the stroke of the cylinder (peak to peak).
R is the radius of the cross-section of the seal.
U is the non-dimensional sliding speed, given by $\mu\omega S/(4ER)$.

The quantity p_o/E cannot be measured directly. However, it can be shown from the Hertzian line contact relationships in [15], that

$$\frac{p_o}{E} = 0.5 \frac{b}{(1-\nu^2)D}$$

where ν is Poisson's ratio ($\nu = 0.5$ for elastomers). Using the soft seal, for which $b/D \cong 0.55$, the ratio p_o/E is 0.37. For the hard seal, for which $b/D \cong 0.52$, the ratio p_o/E is 0.35.

The ratio S/R is the same for both T seals. The value of the ratio is approximately 12.8. The quantity U, for the 10 Hz oscillation frequency, is approximately 18.7×10^{-7} for the soft seal and approximately 9.4×10^{-7} for the hard seal.

Comparison with the plots in [4] shows that run 53 is the closest to the experimental situation. For that run, $\bar{h}_o$ at the 30° BTDC position (wt = 150° in [4]) = 0.1457. Since $\bar{h}_o = (h_o/R)/\sqrt{48U}$, one obtains h_o = 2.74 μm (108 μin.) for the soft seal. For the hard seal, h_o = 1.94 μm (76.4 μin.).

The quantity h_o is the oil film thickness at the center of the contact zone. The above center film thicknesses predicted by run 53 in [4] are considerably greater than those given in Figures 11 and 12. These differences are due in part to the differences between the conditions for run 53 and those that existed experimentally. Consequently, it is desirable to make suitable corrections to the analytical results. These corrections involve the values of p_o/E, S/R, and U.

The effect of p_o/E is considered by extrapolating the analytical results for $\bar{h}_o$ at wt = 150° from runs 51 and 53. The effect of S/R is considered by using runs 55 and 56 to modify these extrapolations. The effect of U is considered by using runs 51 and 52 to further modify the extrapolations.

For the soft seal, the calculation process is:

$$\bar{h}_o \text{ (corrected for } p_o/E) = \left[\frac{0.1457 - 0.1846}{0.25 - 0.1}\right] \cdot (0.37 - 0.25) + 0.1457 = 0.115$$

$$\bar{h}_o \text{ (corrected for } p_o/E, \text{ S/R}) = \left[\frac{0.1823 - 0.2019}{16 - 4}\right] \cdot (12.8 - 8) + 0.115 = 0.107$$

$$\bar{h}_o \text{ (corrected for } p_o/E, \text{ S/R, U}) = \left[\frac{0.2099 - 0.1846}{2\times10^{-6} - 5\times10^{-7}}\right] \cdot (18.7\times10^{-7} - 5\times10^{-7}) + 0.107 = 0.130$$

For the hard seal, the calculations process is similar and produces $\bar{h}_o$ (corrected for p_o/E, S/R, U) = 0.119.

Using the above corrected values of $\bar{h}_o$, h_o for the soft and hard seal are, respectively, 2.4 μm (96.2 μin.) and 1.6 μm (62 μin). These are to be compared with the values of approximately 2.1 μm (82 μin.) and 1 μm (40 μin.), respectively, obtained from Figures 11 and 12. Using the measured values as the reference values, the difference is 17% for the soft seal and 55% for the hard seal.

A comparison of oil film thickness profiles is also of interest. This comparison is provided by Figures 13 and 14. On these figures are reproduced the measured oil film thicknesses of Figures 11 and 12. Also included on each plot is the film thickness profile from run 53 of [4]. For the analytical profiles, the above values of h_o (i.e., 2.4 μm and 1.6 μm for the soft and hard seals, respectively) are used.

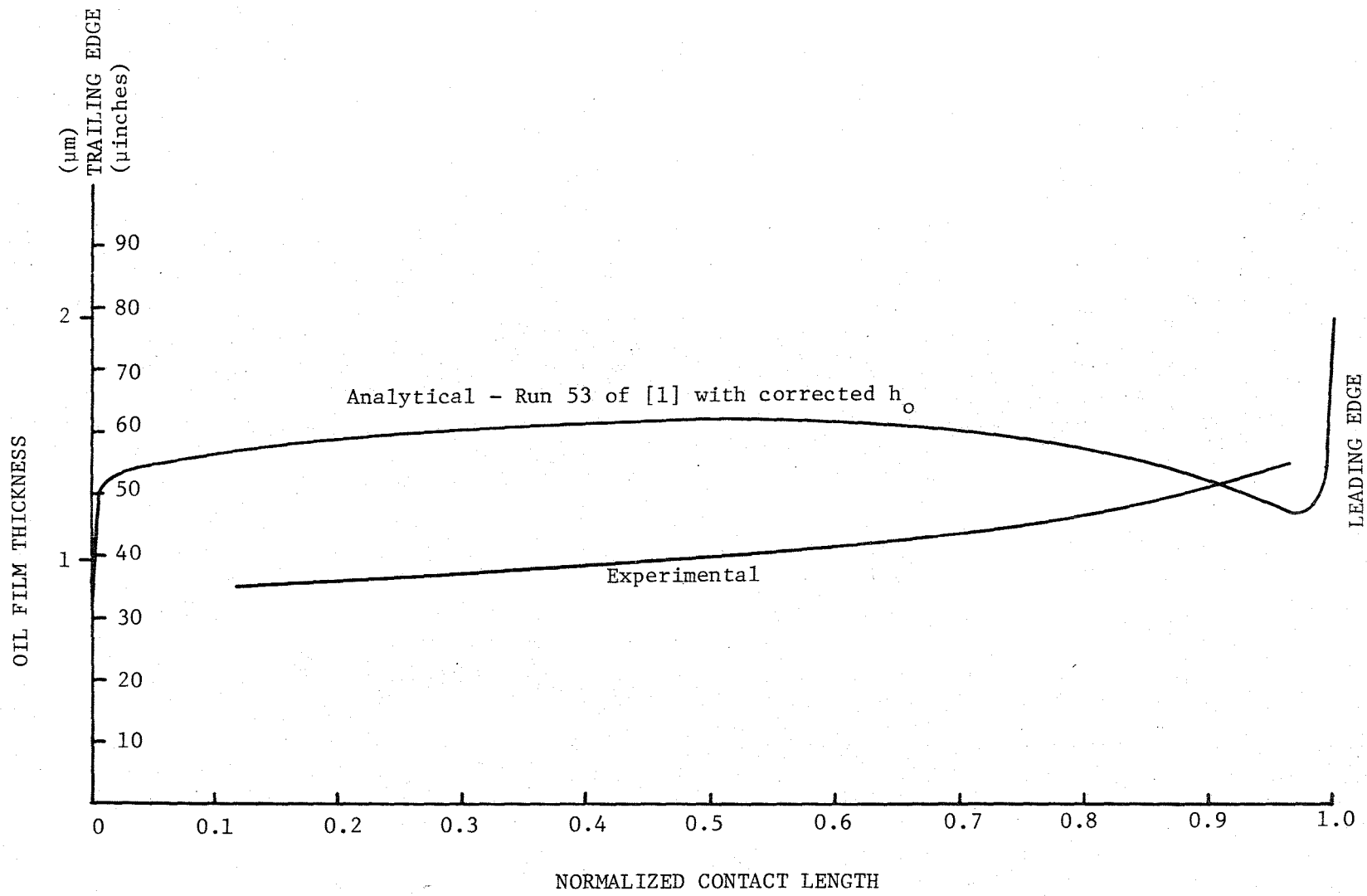

Figure 13 Experimental-Analytical Comparison for Oil Film Thickness (Hard Seal)

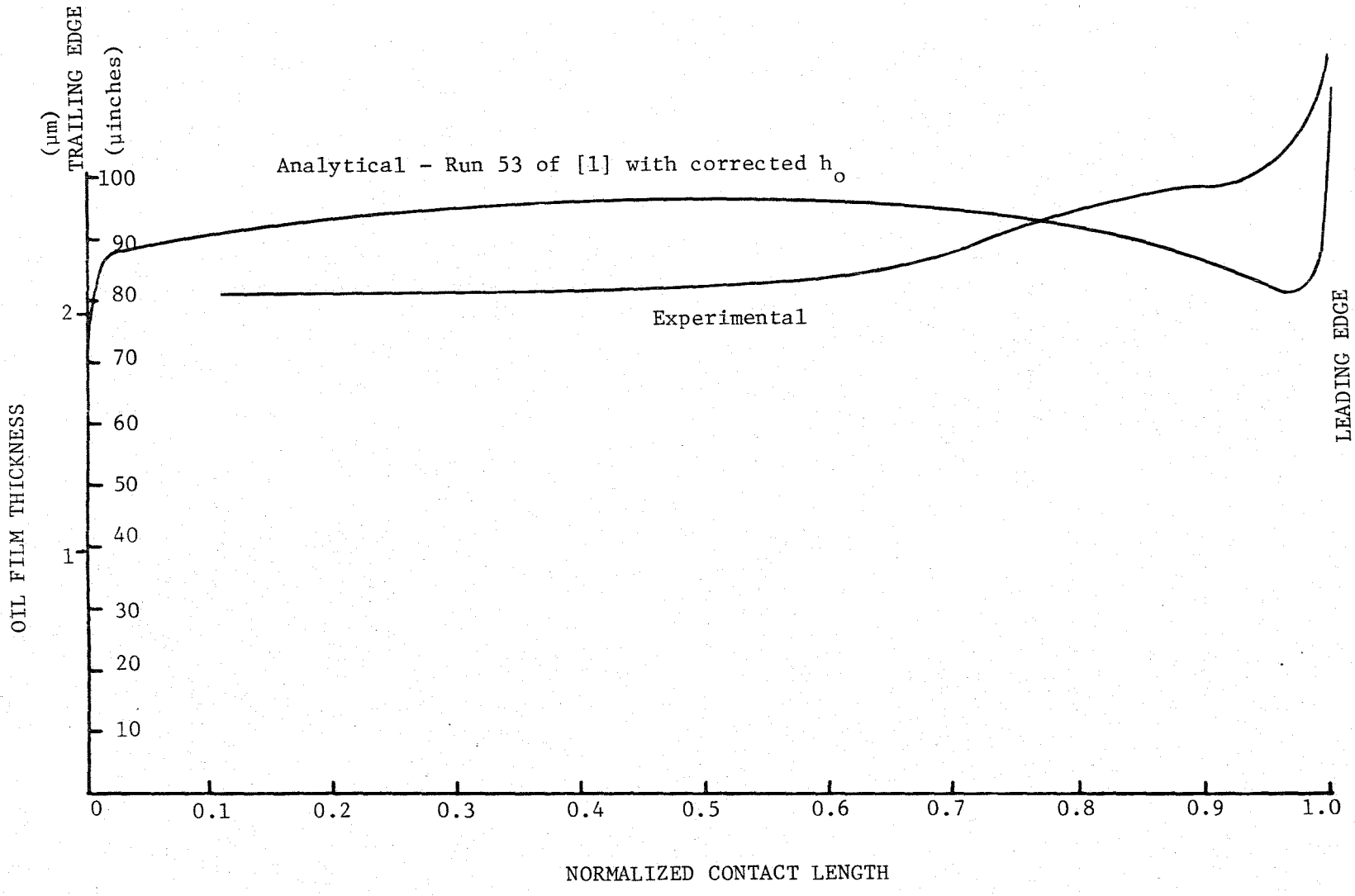

Figure 14 Experimental-Analytical Comparison for Oil Film Thickness (Soft Seal)

Discussion

The results in Table I show that the durometer of the seal has the most significant effect on seal friction. Parameters having a lesser effect are cyclic frequency, preload, and cylinder surface finish. Cyclic frequency has the most important effect on leakage. Seal design is less important. Having even less effect on leakage is seal hardness and cylinder surface finish.

Regarding oil film thickness, only the effect on seal behavior of seal hardness (durometer) was measured. The effect of hardness was considerable -- the film thickness was doubled by decreasing the hardness of the seal from 90 to 70 durometer.

The experimental-analytical comparison for friction force shows that the agreement is not particularly close. Several factors could account for the measured force being greater than that produced by viscous shear effects (Equation (4)). One such factor could be the circumferential variation in the film thickness. The film thickness was measured at only one spot on the seal, and from the photographs in Figure 9, the film thickness distribution is not axisymmetric. The distribution is more axisymmetric for the hard seal case, Figure 8. Correlation of measured and computed forces for the hard seal, therefore, should be and is somewhat better than for the soft seal. However, the improvement in correlation is not sufficient to conclude that circumferential variations in film thickness account for the differences between computed and measured friction force. In fact, for such variations to have produced the lack of correlation would require circumferential oil film thickness variations on the order of 4 to 1. This is highly unlikely.

More likely causes for the lack of correlation include the axial oil film thickness profile (the film does not have a constant thickness as per Equation (4)), dynamic effects due to seal shear deformation and due to oil sloshing outside the contact zone, an error in the flash setting at 30° BTDC, more cyclic film thickness variations than those given by run 53 in [4], force-cell calibration errors, and the actual oil viscosity being different from the nominal in the contact zone.

It is significant that the measured forces are higher than those computed from Equation (4). This suggests that the measured film thickness is unlikely to be greater than those plotted in Figures 11 and 12. Consequently, the use of $i = 1$ for both figures is supported by the above friction force comparison.

Regarding the measured and computed oil film thickness distribution, Figures 13 and 14, only qualitative experimental-analytical agreement

exists*. The soft seal comparison is better, especially in the leading edge region. For neither seal is the trailing edge profile spike observed, although this may well be due to the optical technique being unable to show such a rapidly varying oil film profile.

The separation distance between the seal and cylinder differs, for most of the contact zone, between the analytical and experimental results. This difference was noted above for the center of the contact zone, at which the film thickness h_o exists. Nevertheless, for both seals, there is at least one point in the vicinity of the leading edge where experimental-analytical agreement occurs. This point is at the intersection of the plotted curves.

Many reasons can exist for the differences between the experimental and analytical results for oil film thickness. Some experimental sources of error were discussed above. Analytically, the most likely source is the use of the Hertzian contact pressure profile in the computation of the oil film thickness profile. It is unlikely that this Hertzian profile is appropriate, especially when values of p_o/E in the neighborhood of 0.4 are encountered. Another analytical source is the modeling of the rubber as an elastic material -- in actuality the rubber may exhibit viscoelasticity and/or hysteresis. Such properties, if present in the rubber material, could suppress the existence of the trailing edge oil film spike and reduce significantly the rather abrupt change in oil film thickness that is predicted at the leading edge. Finally, the analysis does not include shear deformation or inertial effects for the elastomeric seal. It is possible that these influences had some effect on the observed oil film thickness.

The experimental-analytical comparisons of the elastomeric seal indicated the need for more work in order to obtain satisfactory agreement between analysis and experiment. Analytically, one major ingredient of this additional work should be to employ a non-Hertzian contact pressure profile in the elastic body portion of the analysis. Another major ingredient is to include viscoelastic effects for the deformation about the preloaded state. Both extensions of the analysis could lead to suppression of the spike in the film thickness profile.

---

*It should be noted that, in the analytical profiles, only h_o is corrected for p_o/E, S/R, and U. The profiles (i.e., the values of oil film thickness not at the center of the contact zone) are not corrected for differences between the values of p_o/E, S/R, and U used in run 53 of [4] and the values that existed experimentally.

Experimentally, additional work should be done to improve the quantity and quality of the interferometric photographs. In the course of the present program, insufficient time was available to perfect the optical procedure, especially as regards seal preparation and production of proper exposures. In addition, insufficient time was available to obtain a large number of photographs, even for the limited number of test conditions that existed. The improvements obtained in photographic quantity and quality would allow more comprehensive and more reliable comparisons with the analysis to be made.

One test condition not treated in the present work is that produced by a non-zero axial pressure gradient across the seal. The present experimental apparatus has the capability for a 690 kPa (100 psi) pressure gradient. Inclusion of this parameter in the analysis and in an associated experimental program would help reveal the nature of seal behavior under conditions more representative of typical elastomeric seal operation.

Since the experimental apparatus, photographic procedure, and analysis are readily applicable to other seal types and materials, such use of these already-developed tools is desirable. One such application is to the scraper seal. This scraper seal has recently become a leading contender in Stirling engine applications despite a lack of fundamental knowledge of its operation. The tools produced in the present program would be very suitable in developing that knowledge. For example, the experimental apparatus, with relatively few modifications, can be employed to obtain interferometric photographs (i.e., oil film thickness measurements) for this seal and to apply a large axial pressure gradient across the seal.

SUMMARY OF RESULTS

This report has presented the results of an experimental-analytical program concerned with the elastohydrodynamic behavior of sliding elastomeric seals for the Stirling engine. During the program, an experimental apparatus was designed and built and a detailed analysis was developed. The analysis determines the instantaneous oil film thickness throughout the cyclic reciprocating motion. The experimental apparatus allows seal leakage, seal friction, and oil film thickness measurements. To obtain the oil film thickness measurement, an optical interferometric procedure was developed.

Tests were run using a fluroelastomeric "T" seal and an "O" ring. Test parameters included cylinder material, cylinder surface finish, seal hardness, cyclic frequency, seal preload, and the time period of the test. The results showed that the durometer of the seal has the most significant effect on seal friction. Other parameters having a measurable effect on seal friction are cyclic frequency, preload, and cylinder surface finish. Cyclic frequency has the most important effect on leakage, with seal configuration having the second most important effect. Of less importance concerning leakage are seal hardness and cylinder surface finish.

Regarding oil film thickness, only the effect of seal hardness (durometer) was measured. The effect of hardness was found to be considerable -- the film thickness was doubled by decreasing the hardness from 90 to 70 durometer.

Experimental/analytical comparisons were made for friction force and oil film thickness. While qualitative agreement was obtained, significant differences exist. These differences include a higher measured friction force and a lower measured oil film thickness than predicted analytically. Differences between the analytical and experimental oil film thickness profiles were also found. Causes for these experimental/analytical differences include the experimental procedure and assumptions in the analytical model -- the most important being the assumed Hertzian contact pressure distribution.

Concluding Remarks

The work has produced a first-time comparison between analytical and experimental oil film profiles for an elastomeric seal in a reciprocating environment. This comparison shows an overall qualitative agreement but indicates that some improvement in the analytical model and in the experimental technique is warranted.

REFERENCES

1. Herrebrugh, K., "Solving the Incompressible and Isothermal Problem in EHD Lubrication Through an Integral Equation," JOLT, Vol. 90, Series F, No. 1, January 1970, pp. 262.

2. Hamrock, B. and Dowson, D., "EHD Lubrication of Elliptical Contacts of Low Elastic Modulus, Part I - Fully Flooded Conjunction," ASME, JOLT, Vol. 100, Series F, No. 2, April 1978, pp. 236-245.

3. Herrebrugh, K., "EHD Squeeze Films Between Two Cylinders in Normal Approach," ASME, JOLT, Vol. 92, Series F, No. 2, April 1970, pp. 292.

4. Krauter, A.I., and Cheng, H.S., "Experimental and Analytical Tools for Evaluation of Stirling Engine Rod Seal Behavior," Interim Report for Contract NAS3-22, Report No. NASA CR-159543, February 1979.

5. "A Collection of Stirling Engine Reports from General Motors' Research - 1958 to 1970, Part 4...Piston Rod Seals," Report No. GMR-2690, General Motors Research Laboratories, Warren, Michigan 48090, April 1978.

6. "A Collection of Stirling Engine Reports from General Motors' Research - 1958 to 1970, Part 5...Piston Seals," Report No. GMR 2690, General Motors Research Laboratories, Warren, Michigan 48090, April 1978.

7. Blok, H. and Koens, H.J., "The 'Breathing' Film Between a Flexible Seal and a Reicprocating Rod," Symposium on Elasto-hydrodynamic Lubrication, Journal of Mechanical Engineers, pp. 221-223.

8. Field and Nau, "The Effects of Design Parameters on the Lubrication of Reciprocating Rubber Seals," 7th BHRA International Conference on Fluid Sealing, Paper C-1, Nottingham, England, September 24-26, 1975.

9. Hirano, F., and Murakami, T., "Photoelastic Study of Elasto-hydrodynamic Contact Condition in Reciprocating Motion," 7th BHRA International Conference on Fluid Sealing, Paper C-4, Nottingham, England, September 24-26, 1975.

10. Roberts, A.D., "Lubrication Studies of Smooth Rubber Contacts," The Physics of Time Traction, Edited by D.F. Hays and A.L. Browne, Plenum Publishing Corporation, 227 West 17th Street, New York, New York 10011.

11. Roberts, A.D., "Optical Rubber," Rubber Developments, Vol. 29, No. 1, 1976, pp. 7-11.

12. Blok, H. and Koens, H.J., "The Breathing Film Between a Flexible Seal and a Reciprocating Rod," Vol. 180, Pt. 3B, Proc. Instn. Mech. Engineers, 1965-1966.

13. Field, G.J. and Nau, B.S., "Optical Interference Method of Studying the Lubrication of a Compliant Bearing," ASME Paper No. 76-LubS-3, May 1976.

14. Schlichting, H., Boundary Layer Theory, McGraw-Hill Book Company, New York, Fourth Edition, 1960.

15. Roark, R.J., Formulas for Stress and Strain, McGraw-Hill Book Company, New York, Fourth Edition, 1954, p. 320, case number 4.

APPENDIX A

BASIC Program for Computing the Oil Film Thickness at the Fringe Overlap Point

APPENDIX A

BASIC Program for Computing the Oil Film Thickness at the Fringe Overlap Point

```
10 INPUT "HARD COPY (1 OR 0)",H          Paper print selection
20 SELECT PRINT 005: IF H=0 THEN 30: SELECT PRINT 215(132)
30 SELECT D
40 READ N,P1,S: P=ARCSIN(SIN(P1/N)): P=COS(P)
50 DATA 1.4605,30,100    Index of refraction of oil, incidence angle, scaling
60 PLOT <0,0,R>                                                  factor for plot
70 FOR K=1 TO 4
80 PLOT <250,0,D>,<0,10,D>,<0,-10,D>
90 NEXT K
100 PLOT <0,0,R>
110 FOR K=1 TO 10
120 PLOT <0,100,D>,<10,0,D>,<-10,0,D>
130 NEXT K
140 FOR J=0.450 TO 0.650 STEP 0.050    Filter frequencies:  0.45-0.65µm in
150 F=J                                                    steps of 0.05µm
160 PRINTUSING 170,"FREQUENCY        FREQ. DIFF.              DISTAN
CE"
170%##########################################################################
###
180 PRINTUSING 170,"(MICROMETRES)  (MICROMETRES)  (MICROMETRES)
 (MICROINCHES)"
190 PRINT
200 FOR I=0.450 TO 0.650 STEP 0.050    Filter frequencies:  0.45-0.65µm in
210 F1=I                                                   steps of 0.05µm
220 IF (F1-F)<1.0E-10 THEN 290
230 D=(F/(2*N))*P*(F/(F1-F)+1)
240 PRINTUSING 250,F,F1-F,D,D*39.37
250%##.#####          ##.#####          ##.#####        ####.#####
260 IF F1-F=.2 THEN 270: Z=0
270 Z=-1
280 PLOT <0,0,R>,<((F1-F)/0.200)*1000+Z,(D*39.37/S)*1000,U>,<0,0
,D>,<0,0,U>
281 PLOT <10,0,D>,<-20,0,U>,<10,0,D>
282 PLOT <0,10,D>,<0,-20,U>,<0,10,D>,<0,0,U>
290 NEXT I
300 D=0.5*(F/N)*P
310 PRINT "FILM THICKNESS CHANGE PER FRINGE WITH THE"
320 PRINT F;"MICROMETRE FILTER IS";D;"MICROMETRES"
325 PRINT "                          OR";D*39.37;"MICROINCHES"
330 PRINT :PRINT :PRINT
340 NEXT J
```

Output of Computer Program

FREQUENCY (MICROMETRES)	FREQ. DIFF. (MICROMETRES)	DISTANCE (MICROMETRES)	(MICROINCHES)
0.4500	0.0500	1.4426	56.7960
0.4500	0.1000	0.7934	31.2378
0.4500	0.1500	0.5770	22.7184
0.4500	0.2000	0.4688	18.4587

FILM THICKNESS CHANGE PER FRINGE WITH THE
.45 MICROMETRE FILTER IS .144262183317 4 MICROMETRES
OR 5.679602354056 MICROINCHES

FREQUENCY (MICROMETRES)	FREQ. DIFF. (MICROMETRES)	DISTANCE (MICROMETRES)	(MICROINCHES)
0.5000	0.0500	1.7632	69.4173
0.5000	0.1000	0.9617	37.8640
0.5000	0.1500	0.6945	27.3462

FILM THICKNESS CHANGE PER FRINGE WITH THE
.5 MICROMETRE FILTER IS .160291320352 6 MICROMETRES
OR 6.310669282282 MICROINCHES

FREQUENCY (MICROMETRES)	FREQ. DIFF. (MICROMETRES)	DISTANCE (MICROMETRES)	(MICROINCHES)
0.5500	0.0500	2.1158	83.3008
0.5500	0.1000	1.1460	45.1212

FILM THICKNESS CHANGE PER FRINGE WITH THE
.55 MICROMETRE FILTER IS .176320452387 9 MICROMETRES
OR 6.941736210512 MICROINCHES

FREQUENCY (MICROMETRES)	FREQ. DIFF. (MICROMETRES)	DISTANCE (MICROMETRES)	(MICROINCHES)
0.6000	0.0500	2.5005	98.4464

FILM THICKNESS CHANGE PER FRINGE WITH THE
.6 MICROMETRE FILTER IS .192349584423 2 MICROMETRES
OR 7.572803138741 MICROINCHES

FREQUENCY (MICROMETRES)	FREQ. DIFF. (MICROMETRES)	DISTANCE (MICROMETRES)	(MICROINCHES)

FILM THICKNESS CHANGE PER FRINGE WITH THE
.65 MICROMETRE FILTER IS .208378716458 4 MICROMETRES
OR 8.203870066967 MICROINCHES

APPENDIX B

Outline of Test Procedure

APPENDIX B

Outline of Test Procedure

Step

1. Install appropriate seal and cylinder as required by the Test Matrix table.

2. Carefully fill the cylinder with Mobil Oil XRL 1032 AR-1 to the designated fill level.

3. Turn on the constant light source (incandescent source).

4. Adjust the microscope and light source to provide a clear, bright image of the seal surface as viewed in the stereo microscope. Focus.

5. Turn on the hydrostatic bearing pump motor.

6. Carefully measure the line width of the seal contact zone, and the width of the groove on the seal holder. Record both measurements.

7. Rotate the flywheel by hand while observing the oil film surface through the microscope.

8. Observe the formation of light fringe patterns as a result of the oil film between the seal and inner cylinder wall surface.

9. If no fringe patterns are observable, repeat procedure from step 4 and refer to optical requirements in Interim Report [1] and in the section entitled Experimental Conditions and Procedures in the present report.

10. Install the desired optical filters (one in front of the front lense on each side of the stereo microscope).

11. Install the microscope camera focusing tube and refocus the images in each eyepiece viewing through the focusing tube.

12. When a satisfactory focus is achieved remove the focusing tube.

13. Load the microscope cameras (2) with Polaroid type 667 coaterless film.

14. Install one of the cameras onto one of the microscope eyepieces taking care not to disturb the position of the eyepiece camera adapter.

15. Suspend the camera by the back clamp from one of the two overhead camera suspension springs. Center the camera by positioning the spring along the back clamp to achieve proper balance of the camera.

16. Install the second camera repeating steps 14 and 15.

17. Switch the constant light source to flash.

18. Adjust the position of the proximity sensors located at the end of the drive shaft to trigger the flash unit at the desired position of the cylinder stroke.

19. Measure oil level.

20. Push the start button. Record start time.

21. Adjust the speed of the motor to the desired frequency for the cylinder.

22. Photograph force gage output from oscilloscope. Record all settings.

23. Open both microscope camera shutters.

24. Push pulse button on the encoder box to trigger the flash. Repeat according to number of flashes desired for proper film exposure.

25. Close microscope camera shutters.

26. Push rig stop button. Record stop time.

27. Remove microscope cameras and extract photographic plates.

28. Measure oil level.

29. Verify that both microscope photographs are acceptable from the standpoints of:

    a. Focus
    b. Exposure
    c. Discernible fringe information

30. If microscope photographs do not meet the desired criteria, repeat steps 3 through 29.

31. Annotate photographs identifying the following:

    a. date
    b. run number
    c. microscope side (left or right)
    d. cyclic position of flash

e. filter used
f. cylinder frequency

32. Repeat all steps for the runs in the Test Matrix table. Eliminate steps 3, 4, 7-18, 23-25, 27, 29-31, for columns 5 through 10 of that table.

1. Report No. NASA CR 165158	2. Government Accession No.	3. Recipient's Catalog No.
4. Title and Subtitle MEASUREMENT OF ROD SEAL LUBRICATION FOR STIRLING ENGINE APPLICATION		5. Report Date July 1980 6. Performing Organization Code
7. Author(s) Krauter, A. I.		8. Performing Organization Report No. SRC-80-TR-62 10. Work Unit No.
9. Performing Organization Name and Address Shaker Research Corporation Northway 10 Executive Park Ballston Lake, NY 12019		11. Contract or Grant No. DEN 3-22
12. Sponsoring Agency Name and Address U. S. Department of Energy Division of Transportation Energy Conservation		13. Type of Report and Period Covered Contractor Report March 1979 - June 1980 14. Sponsoring Agency Code DOE/NASA/0022-2

15. Supplementary Notes
Final Report, Prepared under Interagency Agreement ED-77-A-31-1040
Project Manager: R. E. Cunningham, MS 6-1
NASA Lewis Research Center, Cleveland, Ohio 44135

16. Abstract

This report concerns an experimental and analytical program concerned with the elastohydrodynamic behavior of sliding elastomeric seals for the Stirling engine. During this program an experimental apparatus was designed and built and a detailed analysis was developed. The analysis determines the instantaneous oil film thickness throughout the cyclic reciprocating motion. The experimental apparatus provides seal leakage, seal friction, and oil film thickness. For the oil film thickness measurement, an optical interferometric procedure was developed.

Tests were conducted on commercial elastomeric seals having a 76 mm O.D. Testing conditions included seal durometers of 70 and 90, sliding velocities between 0.8 and 3.6 m/s, and no pressure gradient across the seal. Acrylic and aluminum cylinders and a typical synthetic base automotive lubricant were used.

The work produced a first-time comparison of analytical and experimental oil film profiles for an elastomeric seal in a reciprocating environment. This comparison shows an overall qualitative agreement.

17. Key Words (Suggested by Author(s))		18. Distribution Statement
Seal	Interferometry	Unlimited - UNLIMITED STAR CATEGORY 37 DOE CATEGORY UC-96
Rod Seal	Friction	
Leakage	Stirling Engine	
	Elastomer	

19. Security Classif. (of this report)	20. Security Classif. (of this page)	21. No. of Pages	22. Price*
Unclassified	Unclassified		

* For sale by the National Technical Information Service, Springfield, Virginia 22161

End of Document